Background paper on subsidence monitoring and measurement with a focus on coal seam gas (CSG) activities

Paper prepared for the NSW Chief Scientist and Engineer

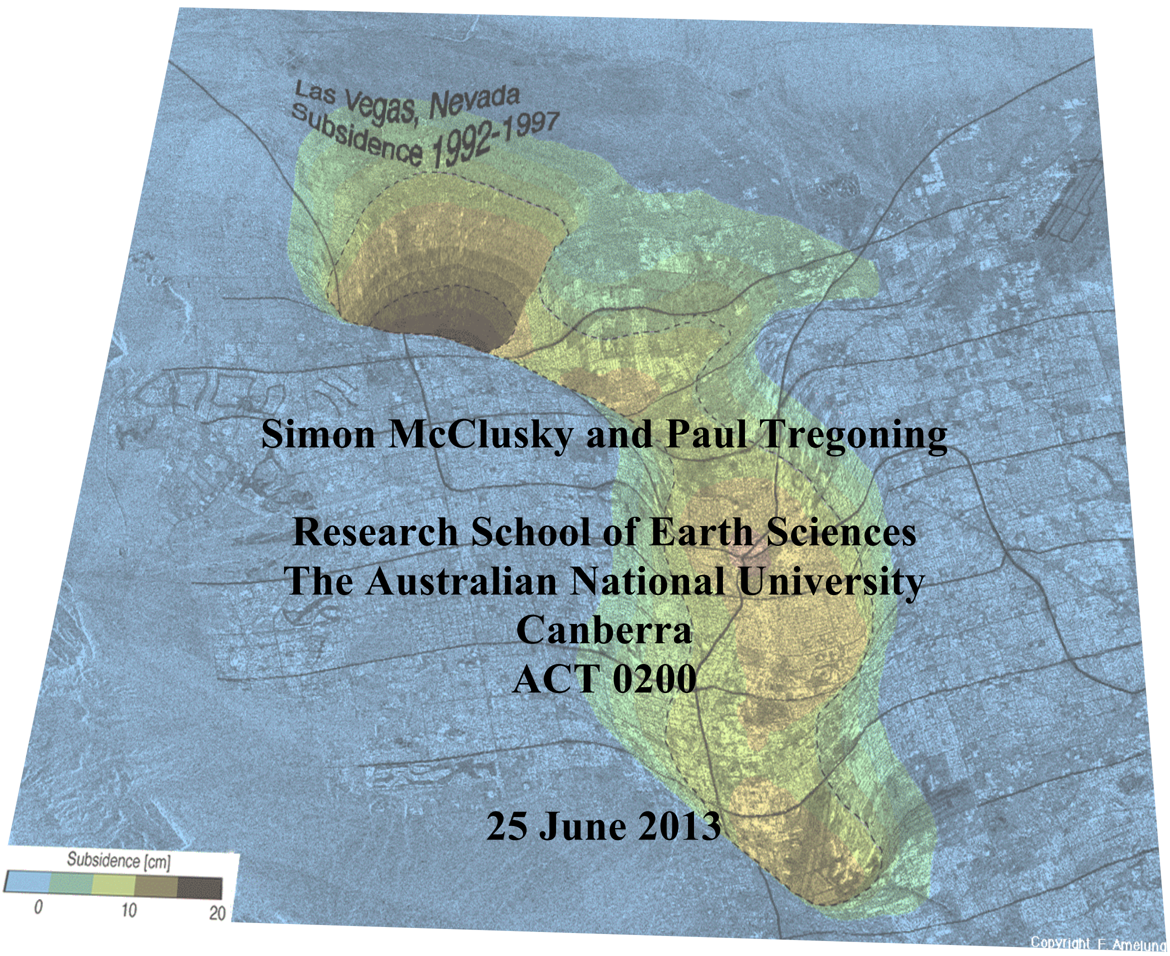

Simon McClusky and Paul Tregoning

Research School of Earth Sciences
The Australian National University
Canberra
ACT 0200

25 June 2013

Cover Image: Subsidence in and around the city of Las Vegas, Nevada, USA due to the withdrawal of groundwater [Amelung et al., 1999]. **Image Credit:** F. Amelung, University of Miami.

Executive Summary

Subsidence is the downward movement of the surface of the Earth relative to some predefined level and the monitoring of subsidence requires detecting changes in the Earth's surface across a region over a period of time.

An issue arising from Coal Seam Gas (CSG) activities is whether the extraction of gas and groundwater causes subsidence at the surface. The purpose of this background paper is to describe the measurement techniques that are available which might be used to monitor regions where CSG activities are either taking place already or are identified for future activities. The question, at its simplest level, amounts to defining the accuracy with which ground deformation can be measured and at what temporal and spatial scales.

Both ground-based and space-based observations can be made to detect changes in the Earth's surface. All require repeat measurements in order to derive estimates of change (i.e. subsidence). The more frequently the observing programme is repeated, the greater the insights will be in terms of how the subsidence pattern evolves over time.

The most appropriate measuring technique for any particular CSG activity monitoring will depend upon the spatial extent of the expected deformation and the likely magnitude. Crude techniques can be used to detect large (i.e. > 0.5 m) deformation signals, while more sophisticated – and more expensive – techniques are required to detect small (i.e. < 1 cm) deformation signals.

A potentially useful side benefit of a careful subsidence-monitoring programme could be that information can be obtained on the nature and propagation of the movement of gas and water at depth below the surface of the Earth. In essence, highly accurate knowledge of the movement of the surface can be used to derive estimates of pressure and volume changes occurring at depth as a result of CSG activities. This information may be of interest to both the mining companies and the Government by providing additional detailed information on how the CSG activities are progressing.

Possible observing techniques

Space-based observations provide a means of monitoring deformation with potentially low levels of involvement of personnel

- Through the use of Global Positioning System (GPS) observations, subsidence at discrete points can be measured with a daily sampling accuracy of < 5 mm. A network of sites needs to be installed across the region of interest and observed repeatedly. It is preferred that the sites would be operated continuously so that the greatest temporal resolution can be achieved.
- For lower-level accuracy, repeat "kinematic"[1] GPS surveys could be undertaken, whereby a series of transects are traversed across a region and the position of the ground is determined as the instrument moves. The accuracy of this approach is 1-5 cm and it requires considerable personnel involvement to cover adequately any moderately sized region.
- Interferometric Synthetic Aperture Radar (InSAR) provides high spatial resolution with an accuracy of 5-15 mm, but relies entirely on the acquisition of imagery from international SAR satellite missions.

[1] Kinematic GPS is an observing technique where the position of a GPS antenna is estimated on very short (ie 1-5 seconds) time scales. It is used to calculate the position of moving vehicles, aircraft etc.

Airborne observation platforms provide flexibility in terms of scheduling observation programmes:

- The use of Airborne SAR removes the dependency on international satellite missions and provides a somewhat higher spatial resolution than satellite SAR, but there is a potential loss of accuracy through poor knowledge of the location and attitude of the aircraft and SAR sensor. Current Airborne SAR systems and differential InSAR (DInSAR) analysis algorithms are still in the research and development phase. The technique, though while very promising is not currently available for use on a commercial basis.
- Airborne LIght Detection And Ranging (LiDAR) involves "pinging" the Earth's surface with laser pulses to determine the distance from the aircraft to the surface. A highly effective method of measuring topography (accurate to 20-100 mm), repeat observations can yield estimates of subsidence. The accuracy of the technique depends on the level of accuracy of the location and attitude of the aircraft.

Ground-based observing programmes can provide estimates of subsidence

- Determining height changes through traditional surveying techniques (e.g. levelling, Electronic Distance Measurement (EDM) height traversing) is time consuming and limited in the spatial extent of the information that it can provide.
- Tilt metres can detect minute surface changes (i.e. ~1 Nano radian) but have instrument drifts that require calibration (which can be achieved when augmented with a GPS network). Commercial enterprises provide off-the-shelf monitoring services (~$40,000/month for a 500 x 500 m region).
- Gravity measurements can provide information about the combined changes in mass beneath a location and the surface deformation that has occurred. This technique is not likely to yield information that warrants the cost and time-consuming fieldwork associated with undertaking the measurements. Space-based gravity observations will not have the spatial resolution needed to make a useful contribution to any monitoring programme.

Baseline measurements

Since subsidence is a measure of change in the Earth's surface, a baseline measurement of where the Earth's surface was prior to CSG activities – or would have been without any CSG activity – is needed. This requires defining the topography of the surface prior to any CSG activity, which in effect means commencing an observing programme in advance of CSG activity.

- For *airborne techniques*, obtaining a baseline measurement simply requires flying an instrument (LiDAR or InSAR) prior to the CSG activity.
- For a *continuous GPS monitoring network*, sites will need to be installed for 1-6 months prior to the commencement of CSG activity. The advance time is required to enable accurate characterisation of the natural variability of surface in the region (if detection of sub-cm deformation is required)
- For *ground-based observations*, instruments and/or reference marks will need to be installed and observed at least once prior to CSG activities.
- For *space-based InSAR*, SAR images will need to be either available or their acquisition scheduled prior to CSG activities. In addition, very specific restrictions on the time interval and the "baseline" (the difference in position of the satellite at the time of taking images) must be met for images prior and subsequent to CSG activities for deformation estimates to be derived from the imagery.

For the first three techniques above, deriving a baseline measurement requires only the commitment of resources to either make the observations or install the appropriate equipment. Only the space-borne InSAR technique poses technical/logistical problems in terms of generating baseline measurements, because of the current lack of operational InSAR missions; hence, the inability at the present time to acquire pre-activity imagery of specific regions. Two SAR missions are scheduled for launch in late 2013 and, if successful, this risk would be mitigated.

What subsidence can be detected?

Most accurate: It is possible to detect subsidence of as little as 1-3 mm using continuous GPS, but this technique provides information at only discrete points where the equipment is installed.

Spatial resolution: Space-based InSAR, airborne LiDAR/InSAR provide the greatest spatial resolution, covering up to hundreds of kilometres. The accuracy of the techniques ranges from 5 – 100 mm, largely governed by the accuracy of the modelling of the atmospheric effects (space-borne) and estimates of the location of the aircraft (airborne).

Temporal resolution: Ground-based, continuously operating instruments provide the greatest temporal resolution of any monitoring programme. Tilt metres provide sub-daily estimates of changes in the surface, and can quantify the instantaneous impact of any specific activity. Continuous GPS is typically used to provide daily estimates of position change. However, the information from both techniques is only available at discrete points.

Recommended approach to monitoring subsidence

1. Airborne differential InSAR is the technique with the promise to deliver the optimal spatial and temporal resolution with sufficient accuracy to measure subsidence and with the best flexibility in terms of scheduling observations. However, we are not aware of this technique having been used previously in Australia, nor of any in-country capability to undertake such monitoring.

2. For small- to moderate-sized monitoring programmes (500 m – 100 km), a combination of continuous GPS and differential InSAR would yield the most cost-effective approach, while yielding subsidence estimates with an accuracy of 10-20 mm.

3. The addition of tilt metres over small areas (500 x 500 m) would further increase the accuracy and would also enable the propagation of subterranean changes in gas/water reserves to be monitored.

4. A pilot study could be undertaken in the southern Sydney/Campbelltown region where existing GPS and SAR imagery exists over a spatial region where CSG activities have been underway over the past decade. This would allow the quantification of subsidence that has already occurred, as well as a demonstration of the capability of space-borne techniques to detect and monitor subsidence related to CSG activities.

Table of Contents

1. Introduction

Subsidence is, by definition, the downward movement of the surface of the Earth relative to some datum. It is essentially just a measurement of movement of the surface in a particular direction; therefore, any observation/measurement technique that can detect movement of the Earth (often called “deformation”) might be employed to measure and monitor subsidence.

The most appropriate technique and observing procedure for measuring subsidence will depend on the spatial extent of the anticipated deformation and, perhaps more importantly, the likely magnitude of the expected subsidence. Some techniques (e.g. continuous Global Positioning System - GPS observations) can provide highly accurate temporal estimates of surface movement but are expensive to maintain, and deliver only spatially discrete estimates. Other techniques (e.g. Interferometric Synthetic Aperture Radar - InSAR) provide greater spatial resolution but lower accuracy and temporal resolution. For logistical and cost reasons, terrestrial measurement techniques are best suited to only small local regions.

In the case of monitoring subsidence that may be related to coal seam gas activities, what is of interest is the location of the surface relative to where it was before any CSG activity commenced, or where the surface would be had no CSG activity been undertaken. Thus, inherent in any subsidence monitoring programme is the need to separate deformation related to subsidence from any other sources of movement of the surface. This processes is know as establishing a “zero baseline” observation, or “baseline” measurements and is an important component of any monitoring programme.

There are, in fact, several reasons why the location of the surface of the Earth changes with time that may have nothing to do with subsidence related to CSG activities. For example, changes in the mass of the atmosphere can cause uplift or subsidence of the surface by as much as 10-15 mm, although the mean deformation would be zero over several years. However, measuring surface heights at only discrete times could lead to incorrect quantification of subsidence rates if other geophysical processes are not properly accounted for. Other geophysical processes that are known to cause surface deformation and have been detected in Australia through measurements include hydrological loading [e.g. Tregoning et al., 2009], earthquake deformation [e.g. Tregoning et al., 2013] and interseismic/postseismic tectonic strain accumulation.

This report describes observing techniques that are capable of quantifying subsidence over a range of spatial and temporal scales. We explain how the observing techniques work, how they are applied to monitoring subsidence and the strengths and weaknesses of each technique. In some cases, realistic estimates of indicative costs are provided, although it was beyond the brief of this report to fully cost any actual monitoring scheme and we have not sought actual commercial quotes for any monitoring activities.

The most suitable approach for monitoring subsidence of a particular region will depend on several factors, with the two most likely to govern the choice of approach of monitoring being the spatial extent of the anticipated deformation field and the expected magnitude of the anticipated deformation. Both of these will be related to how much gas extraction and water injection/extraction will occur – and at what depth. This information was not available at the time of writing this background paper; therefore, we have restricted our discussions of subsidence monitoring related to CSG activities to the more general level of monitoring subsidence from any cause and of any magnitude.

2. Different Methods used for measuring and monitoring subsidence

2.1 Satellite Monitoring

2.1.1 Global Positioning System (GPS)

The Global Positioning System, commonly known as GPS, is a US military satellite navigation system that was developed to provide precise positioning and navigation capability to the US military. Since its inception, it has found far wider use and application than its original intention. Today, many vehicles, agriculture and mining infrastructure and even many mobile phones either provide or rely upon positioning using GPS.

The scientific community realised many decades ago the potential of GPS to measure very accurate changes in position, and GPS quickly became a scientific tool that was used to study plate tectonic motion, deformation caused by earthquakes, stability of infrastructure (such as mines, dams, bridges) and land subsidence.

2.1.1.1 How does GPS work?

The GPS comprises a constellation of satellites in 6 orbital planes, circling the Earth at ~20,000 km altitude, as well as ground-based tracking stations for either uploading new information to the satellites or for receiving transmitted signals from which their location can be determined.

There are three main ways in which users can obtain positioning information from GPS: navigation mode, kinematic mode and precise-positioning mode. Each of these has a different level of accuracy and, therefore, is suitable for different applications. While we describe briefly below the three modes, it is really only the precise-positioning mode that will deliver the requisite accuracy for directly measuring and monitoring subsidence at the 1-10 millimetres (mm) level.

- Navigation mode:
  Most civilian users are familiar with GPS through its navigation mode, whereby a simple GPS receiver/antenna converts the signals from 4 or more satellites into an estimate of the location of its antenna. This is the mode used in car navigation systems, mobile phones and aircraft, and provides instantaneous positions with an accuracy of 1-5 metres (m). The satellites transmit information regarding:
  a) Where they are,
  b) When they transmitted the message,
  c) The offset of their satellite clock with respect to what is known as "GPS time"[2].

  The GPS receiver decodes the transmitted information and records the time of reception, based on its own clock. The difference between the time of reception and time of transmission, multiplied by the speed of light is a measure of the distance between the GPS antenna and each satellite. The position of the GPS antenna (and the offset of the receiver's clock from GPS time) is calculated by solving the "navigation equations" which describe the simple geometrical

[2] GPS time is the basis of the whole GPS system. It was zero at 0h 06 January 1980 and is currently 16 seconds ahead of UTC. Because no clock will ever run perfectly at the rate of GPS time, the difference of satellite and receiver clocks from GPS time is quantified and known as a "clock offset".

distance relationship between the satellites and GPS receiver on the ground. Since the GPS receivers' clock is not synchronized to the GPS time standard kept by precise atomic clocks on the satellites, an additional receiver clock offset must also be estimated along with the three dimensional (3D) position of receiver. For this reason the navigation mode GPS method requires the simultaneous observation of at least 4 satellites since to solve for 4 unknowns (latitude, longitude, height and a receiver clock offset) requires 4 distance observations.

The accuracy of the navigation mode is controlled by the geometry of the satellites above the receivers' horizon, and the accuracy of the information related to the satellite orbits and clock offsets uploaded to the GPS satellites by the ground segment of the GPS system. If the satellites transmit low-accuracy location and clock information then the accuracy of the navigation mode will decrease. This is why a broad range of 1-5 m accuracy is often quoted for positions derived using the navigation mode of GPS.

- <u>Precise Positioning mode</u>:
  In this mode, the phase of the signals transmitted by the GPS satellites is used, rather than just the transmission time information that is modulated onto the transmitted signals and used in the navigation mode described above. Through a sophisticated analysis processes, it then becomes possible to estimate not only the location of the GPS antenna that has recorded the incoming phase measurements but also the locations of the satellites themselves (and their respective clock offsets with respect to GPS time). This overcomes the potential inaccuracies inherent in the navigation mode, being imprecise knowledge of the locations of the satellites and when they transmitted the signals, but come at the cost of not being able to produce position estimates in real-time.

  Using precise positioning mode, it is possible to derive the location of a stationary GPS antenna with an accuracy of ~5 mm from 24 hours of continuous observations of the GPS satellite constellation. Then, with measurements separated in time, changes in position can be detected. With continuously operating receivers, it is possible to estimate the linear motion of sites with an accuracy of ~ 0.2 mm/year, as has been shown recently across the Australian continent [Tregoning et al., 2013].

- <u>Kinematic mode</u>:
  For users requiring real-time positioning accuracy greater than that, which can be obtained from the navigation mode, it is possible to improve upon the navigation position by applying some real-time corrections to the measurements made by the GPS receiver. In the simplest case, a "block shift" of position can be applied, being the difference between the known coordinates of a nearby point and the coordinates derived from the navigation mode. If such information is broadcast to and applied by other GPS receivers in a local area then the accuracy of the navigation mode can be improved to perhaps better than 1 m.

  Alternatively, positions can be calculated from differences in phase measurements between two GPS receivers, resulting in real-time accuracy of a few centimetres (cm) provided the two receivers are not separated by more than ten's of kilometres (km).

To detect subsidence of several centimetres or less, either precise positioning or kinematic mode GPS would deliver estimates of position with sufficient accuracy to detect the deformation signal. To obtain accuracy greater than 2 cm, post-processed precise positioning would be required.

To achieve the highest levels of accuracy (i.e. < 10 mm) for the position estimates there are many factors that must be taken into account when processing the GPS phase observations. For example,

- changes in the Earth's atmosphere affect the time taken for the signals to travel from satellite to ground-based receivers,
- the ebb and flow of the ocean tides causes increase/decrease in ocean mass on the continental shelf which, in turn, causes deformation of the surface even hundreds of kilometres away from the coast,
- changes in atmospheric pressure and soil moisture/groundwater cause movement of the surface of the Earth,
- precise modelling of the orbits of the GPS satellites is required in order to estimate accurate site coordinates,
- an accurate representation of the coordinates of global GPS tracking sites is required in order to estimate accurately the orbits of the GPS satellites

Readers are referred to Tregoning and Watson [2009] and Tregoning et al. [2013] for further details on analysis strategies that will deliver position estimates in Australia of the requisite accuracy for detection of subsidence.

2.1.1.2 Approach to using GPS to measure subsidence

Kinematic GPS: This technique requires at least two GPS receivers. One is fixed and operates at a known location while the "rover" receiver moves across the region of interest, profiling the ground in a series of transects. Depending on the size of the region to be monitored, the roving antenna can be hand-carried, mounted on an all-terrain vehicle or mounted on a vehicle. The height of the roving antenna relative to the fixed system is estimated and, if the transects are measured repeatedly over a period of time, changes in surface height can be determined.

Precise Positioning GPS: This technique requires specific locations to be observed repeatedly, either through a schedule of observations or through continuous operation of the GPS receivers. The antennae must be placed in exactly the same location each time the point is measured. This is typically accomplished through either the construction of pillars or the installation of fixed mounting points (e.g. bolts) into rock. The monument to which the antennae are fixed must move with the surface of the ground so that any change in position of the antenna reflects and can be interpreted as a change in surface height.

Knowing that crustal deformation of up to 2 cm can occur as a result of processes not related to CSG activities (e.g. surface and groundwater variations, atmospheric pressure changes), discrete temporal measurements may not provide the accuracy of position estimates required to detect sub-cm subsidence. In addition, it is well documented through the operation of the global network of sites by the International Global Navigation Satellite Service (GNSS) that even changes in equipment at continuously operating sites can cause discrete changes in position, even if the position of the monument hasn't actually changed. Such equipment-related changes are detectable in time series of positions derived from continuously operating instruments [e.g. Tregoning et al., 2013] but will not be separable from deformation signals in the case of sites observed sporadically.

2.1.1.3 Strengths and weaknesses of GPS

There is abundant evidence of the use of GPS to detect and quantify crustal deformation, including subsidence, uplift and crustal deformation before, during and after earthquakes. In Australia, precise positioning GPS has been used to identify, for example hydrological loading [Tregoning et al., 2009], subsidence due to groundwater extraction [Featherstone et al., 2012], deformation caused by earthquakes [Watson et al., 2012; Tregoning et al., 2013] and subsidence due to mining [e.g. Ng et al. 2010]. For example, subsidence of ~40 mm over 2000-2008 is seen (Figure 1) in our time series of height estimates at a GPS site near Perth, WA (IGS site code PERT), which has been attributed to the extraction of groundwater from the Yarragadee aquifer that commenced in 2000 [Featherstone et al., 2012].

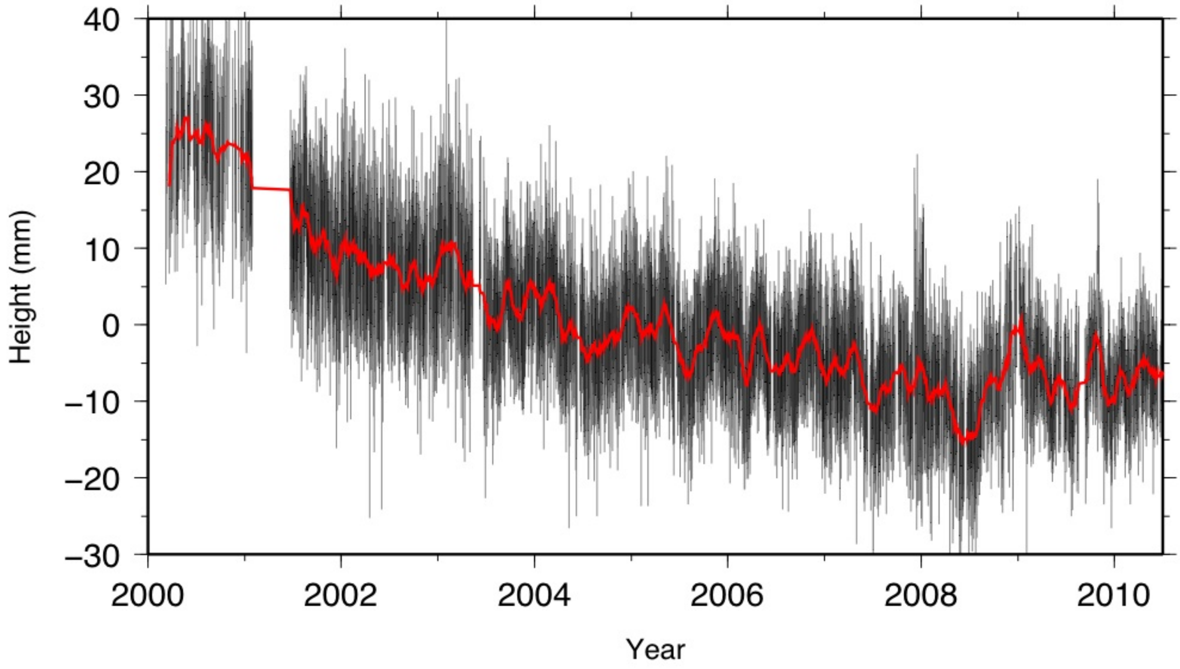

Figure 1. Time series of height estimates (and 1-sigma uncertainties) from our analysis of 10 years of GPS observations at Perth, Western Australia. The non-linear subsidence is related to groundwater extraction [Featherstone et al., 2012]. Red line is a 30-day running average.

Main strengths of GPS

- The ability to detect mm-scale movements provided a post-processing approach is used and analysis strategies are optimised to account for all known temporal variations that affect the GPS signals.
- Can also provide estimates of the water content of the troposphere, which can then be assimilated into Inrerferometric Synthetic Aperture Radar (InSAR) analysis to improve the accuracy of the results (see Section 2.1.2.2).
- Can provide continuous temporal monitoring

Main limitations of GPS

- Requires significant fieldwork and human resources if repeat kinematic GPS surveys are to be conducted.
- Provides information at only discrete locations if continuously operating sites are installed.
- Relatively expensive to install and operate a continuous network of GPS sites, but greater insights would be gained from a spatially dense network.

2.1.2 Synthetic Aperture Radar Interferometry

Satellite Interferometric Synthetic Aperture Radar[3] (InSAR) is an innovative and cost-effective tool for remotely measuring the deformation of the ground and man made structures from space.

[3] RADAR is an acronym for **RA**dio **D**etection **A**nd **R**anging coined in 1940 by the US navy. Radar is a sensor system that uses radio waves to determine the range, direction and speed of objects.

Synthetic Aperture Radar (SAR) sensors onboard Earth Observing Satellites (EOS), orbiting at altitudes of 500 - 800 km above Earth, are capable of imaging large areas (1000s of square kilometres) on a frequent basis (every 5 – 30 days). Through InSAR processing of satellite SAR imagery it is possible to infer ground stability over time of regions as small as 20 square metres. InSAR analysis is both a commercial and scientific technique used to study phenomena such as deformation caused by earthquakes, stability of man-made infrastructure (e.g. buildings, cities) and ground subsidence.

2.1.2.1 How does Synthetic Aperture Radar work?

SAR is a microwave imaging technique invented in June 1951 by mathematician Carl Wiley [Wiley 1985]. At the most basic level, SAR is a technique for improving the spatial resolution of radar observations using multiple images of a specific target collected from a moving platform. Operating in the X-, C-, and L-band microwave frequencies (300 GHz to 300 MHz, equivalent to wavelengths of 1 mm – 1 m), SAR systems provide images representing the electrical and geometric properties of the Earth in all weather conditions. Since they provide their own electromagnetic illumination, SAR instruments can operate in the daytime or at night. SAR images are collected by transmitting a series of coded microwave pulses from a moving antenna that illuminates a swath on the ground that is offset from the flight ground path of the observing platform (in this case a satellite) (Figure 2).

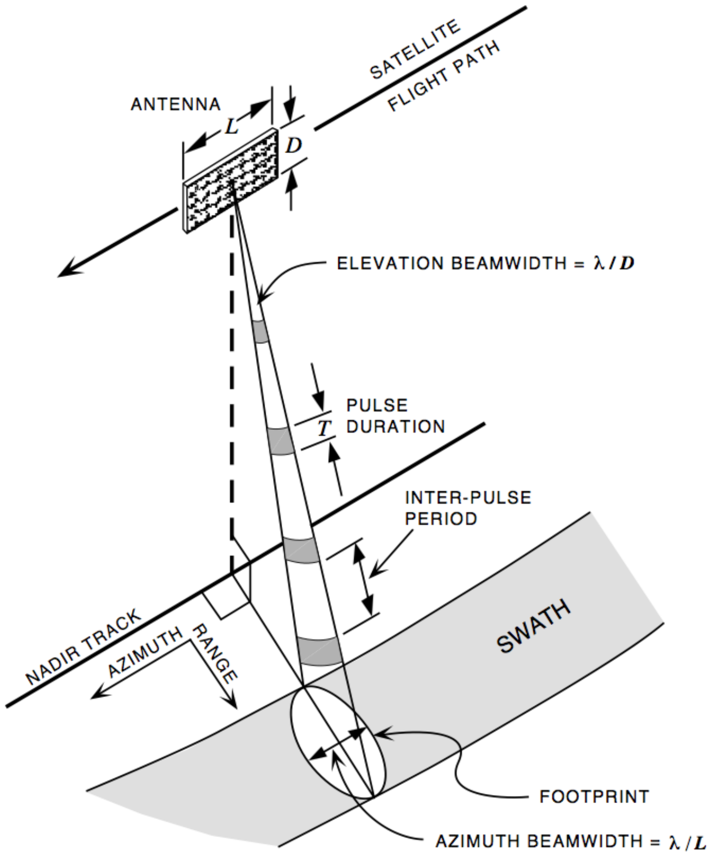

Figure 2. A typical imagining scenario for a SAR system. The platform carrying the SAR sensor is moving in the "along-track" or "azimuth" direction. The radar antenna, with physical dimensions L x D points to the side, imaging the terrain below. Distances or "ranges" are measured across the radar "footprint" to the ground surface in the "look" direction also known as the "cross-track" or "range" direction. The area swept out by consecutive radar measurement "footprints" is known as a "swath". **Image Credit:** [*Olmsted C., 1993*].

The reflected pulses or echoes are recorded between the transmission events. The technique is know as SAR because in the along-track, or azimuth direction (see Figure 2) a large virtual aperture is formed by coherently combining a collection of reflected radar pulses received as the radar moves along in its flight path. Therefore, although a typical radar antenna of a SAR instrument has a physical size on the order of metres, the synthesized SAR antenna aperture can be on the order of kilometres. The wide synthetic aperture formed by space-borne sensors enables SAR images to be collected with typical ground resolutions on the order of 5 – 25 metres per pixel and swath widths of 10s to 100s of kilometres, depending on the particular instrument and mode of operation. Typical individual SAR satellite images cover areas of 100 to 1000 square kilometres.

Satellite-based Interferometric Synthetic Aperture Radar, commonly referred to as InSAR, is the geodetic SAR processing technique developed in the early 1990s that uses two or more SAR images to generate maps of topography and/or deformation of the Earth's surface [Massonett & Feigl, 1998; Burgman et al., 2000; Bamler and Hartl 1998; Ferretti et al. 2001; Hanssen 2001; Kampes 2006; Simons and Rosen 2007; Prati et al. 2010; Hooper et al. 2012]. Using the differences in the phase of reflected radar signals from two different satellite passes over the same place on the Earth's surface, it is possible to make precise millimetre-scale measurements of changes in ground deformation over time spans of days to years. Figure 3 illustrates the technique; if the distances between the repeat SAR satellite observations of a specific point on the Earth surface are the same, then the phase of the reflected signal will also be the same. Should this distance change, however, either through the motions of the satellite or from the deformation of the Earth surface, then the phase of the reflected signal will change by an amount equal to the change in distance modulo the wavelength of the microwave signal used to make the measurement. If there is accurate knowledge of the position of the satellite in its orbit, then the amount that a region of the Earth surface moves in a given period of time may be calculated by measuring the shift in the phase of the microwave signal reflected from that region (often called a "pixel").

Based on this principle, measurements of the phase change at thousands of pixels on the Earth surface are used to produce an InSAR image, or differential interferogram. The method of extracting ground deformation form InSAR images of the Earth is commonly referred to as differential InSAR (DInSAR). DInSAR has the great advantage of enabling deformation of large swaths of the Earths surface to be measured with little or even no ground instrumentation.

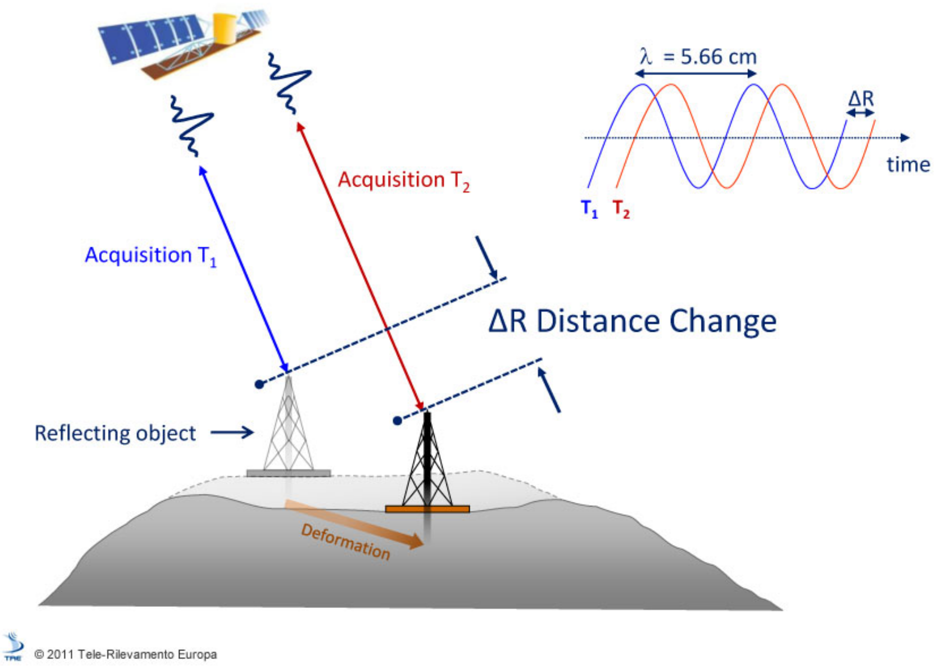

Figure 3. Relationship between ground movement and the corresponding shift in signal phase between two SAR signals acquired over the same area at different times. **Image Credit: [**http://www.treuropa.com]

Figure 4 shows a series of DInSAR interferograms imaging an oil field in California. In this image, the time evolution of land subsidence associated with oil extraction over a 4 year period is shown. Some of the drawbacks and complications in generating such images of deformation include image decorrelation, atmospheric interference and satellite look angle and terrain slope limitations. These complications are discussed in some detail below in section 2.1.2.2

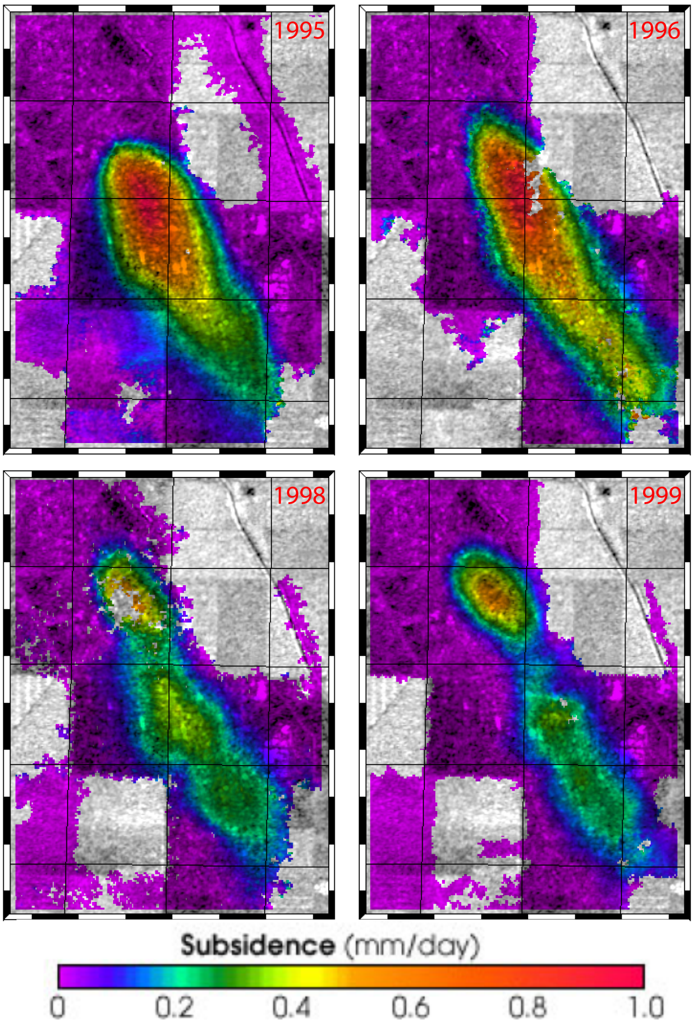

Figure 4. This figure shows a comparison of SAR interferograms from four different years mapping the rapid ground subsidence over the Lost Hills oil field in California. Lost Hills is located about 60 km NW of Bakersfield in the San Joaquin Valley. The oil field is about 1.5 km wide and 6 km long. Each SAR interferogram was created using pairs of images taken by SAR that have been combined to measure surface deformation or changes that may have occurred in the time between when data for the two images were taken. SAR images were collected by the European Space Agency's Remote Sensing satellites (ERS-1 and ERS-2) in two months of each year shown (1995, 1996, 1998 and 1999). The DInSAR measurements show primarily subsidence of the surface, are rendered in colour with purple indicating no motion and the brightest red showing rapid subsidence of about 36 centimetres per year. The white areas are where the radar measurements could not be obtained, mostly in the agricultural fields around the oil fields where plant growth or ploughing altered the radar properties of the surface. These radar data show that parts of the oil field were subsiding rapidly at more than 3 centimetres per month, in 1995 and 1996. **Image Credit:** NASA/JPL.

2.1.2.2 Approach to using InSAR to measure subsidence

Single interferogram Differential InSAR methods for measuring deformation were first developed in the early 1990s and are commonly referred to as conventional DInSAR techniques, [Massonnet et al. 1993; Peltzer and Rosen 1995], these techniques have evolved rapidly over the last two decades into advanced DInSAR techniques which provide information not only on the spatial distribution of deformation, but also the temporal evolution of the ground deformation over time. Under favorable conditions these advanced DInSAR techniques are capable of theoretically making millimetre-level precision measurements of line-of-sight[4] ground deformation using long time series of interferometric SAR image data over time spans of months to a decade or more. The

[4] "Line-of-sight" deformation refers to the change in Earth's surface in the direction that the satellite radar was looking. This can be converted into horizontal and vertical components on the ground, but InSAR studies often simply analyse and interpret the line-of-sight changes themselves.

conditions or circumstances, that limit the precision or the availability of useful data for DInSAR usage, are discussed briefly below and in detail in section 2.1.2.3.

According to Sansosti et al. [2010], advanced DInSAR techniques can be grouped into two main categories:

1. Persistent Scatterer (PS) methods that identify and integrate the position of individual points that act like point scatterers, that is pixels that have coherent phase and stable amplitude properties across all interferograms within a particular time period with respect to a common master scene [Ferretti et al. 2001; Werner et al. 2003],
2. Small BASeline or SBAS methods, that use an optimized set of interferograms selected to minimize both the temporal and spatial interferometric baselines providing a time series of deformation for any consistently phase coherent pixel in the combined InSAR image stack [Lundgren et al. 2001; Berardino et al. 2002; Mora et al. 2003; Schmidt and Burgmann 2003; Prati et al. 2010].

While somewhat different in their approach to the analysis of the raw SAR data, both of these advanced DInSAR techniques, and their multiple variants, enable monitoring ground deformation in a particular region through time on a regular or quasi-regular basis. The SAR images acquired at different dates, across the time window of interest, are combined in pairs to generate a set of differential interferograms that contain information on the interferometric phase (Φ_{int}). For monitoring ground deformation or subsidence, these InSAR images should contain only the ground displacement that occurred between the acquisition times of the two SAR images (Φ_{def}). However, in practice, there are other terms that contribute to interferometric phase that contaminate the ground displacement information. The fundamental objective of all DInSAR processing techniques is to accurately extract the ground displacement term from the remaining components. The interferometric phase can be expressed as the sum of the following terms [Hanssen 2001]:

$$\Phi_{int} = \Phi_{def} + \Phi_{topo} + \Phi_{orbit} + \Phi_{atmos} + \Phi_{noise} \qquad (1)$$

Φ_{topo} is the topographic contribution to measured phase, Φ_{def} is the phase contribution due to ground deformation occurring between the two SAR image acquisitions, measured along the line of sight (LoS), Φ_{atmos} is the phase component due to atmospheric disturbances – in particular the variable water content, Φ_{orbit} is the phase component caused by errors in positioning of the satellite at each observation epoch and Φ_{noise} includes the remaining noise sources. The Φ_{topo} contribution to equation (1) can be extracted or removed from the Φ_{int} phase using a Digital Elevation Model (DEM) of the region. The global Shuttle Radar Terrain Model [Farr et al., 2007; Rodriguez et al., 2005] known as the SRTM DEM has sufficient accuracy for this purpose, and is available for most regions of the Earth except the extreme polar areas above and below about 60 degrees latitude. The atmospheric delay component, Φ_{atmos}, can be accounted for using estimates derived from global numerical weather models or by using estimates of tropospheric water vapour from nearby GPS networks. The latter has been shown to be effective in mitigating atmospheric delay errors in InSAR analyses [e.g. Wadge, et al., 2002; Williams, et al., 1998; Xu et al., 2006]

Expected results

DInSAR techniques can provide a great deal of information on the distribution, magnitude, and changes over time of ground subsidence. The methods described above provide the means to accurately monitor satellite-to-ground “Line-of-Sight” (LoS) changes over time. These LoS measurements are generally represented as maps showing the spatial distribution of LoS displacement, either as an average rate or as an accumulated displacement. The former corresponds to the average displacement rate over the period of time spanned by the processed SAR images are processed, expressed in millimetres per year (mm/yr) or centimetres per year (cm/yr) [see Figure

5b], whereas the latter is the total amount of subsidence with respect to the first SAR acquisition, usually expressed in mm or cm [Figure 5a].

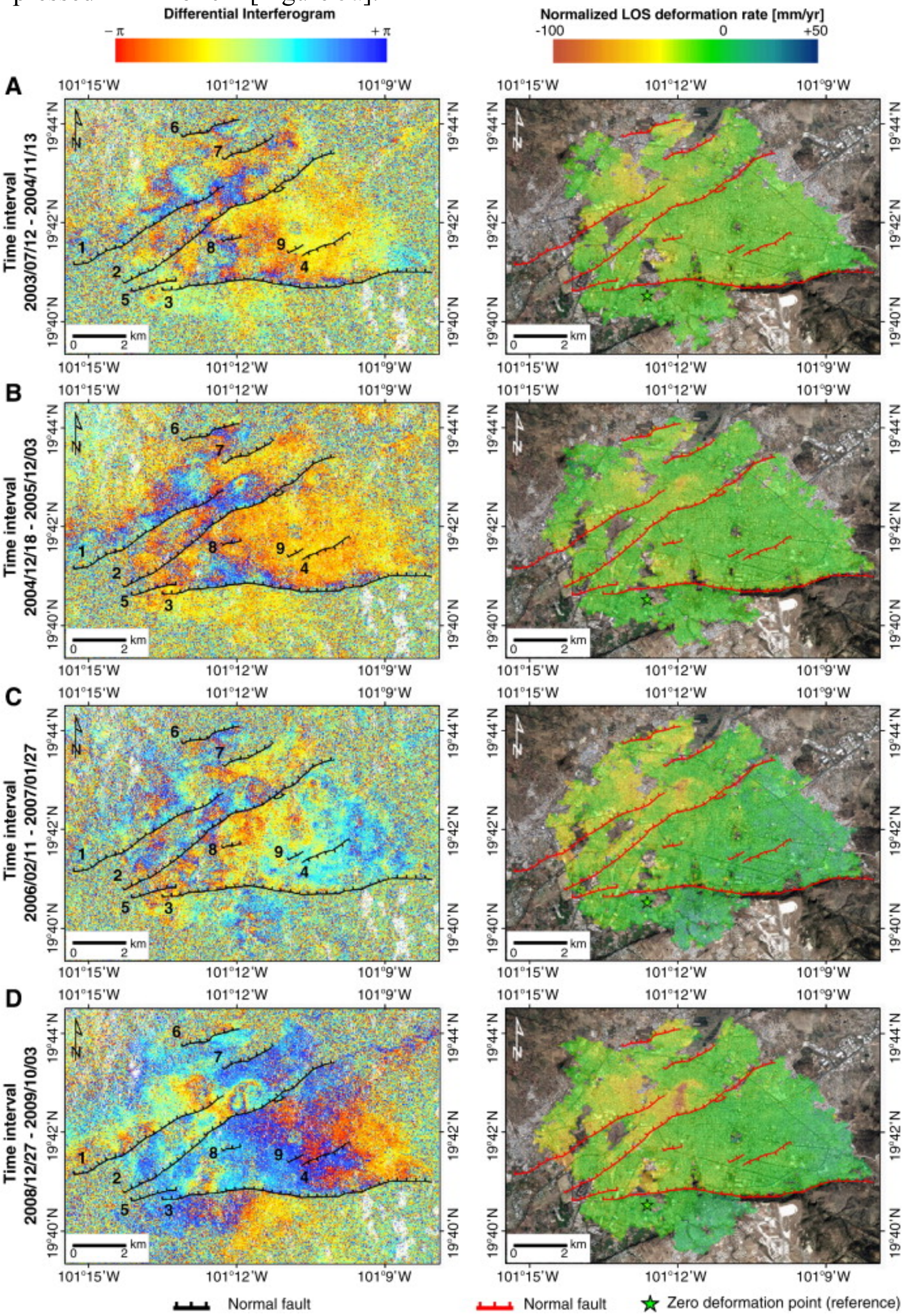

Figure 5. Temporal evolution of LoS deformation rates for the Morelia region in Mexico showing subsidence related to water withdrawal between 2003 and 2009: **a)** ENVISAT differential interferograms "wrapped" are shown in the left column and **b)** "unwrapped" LoS deformation rates are shown in the right column for SAR pairs A (12 Jul 2003–13 Nov 2004), B (18 Dec 2004–3 Dec 2005), C (11 Feb 2006–27 Jan 2007) and D (27 Dec 2008–3 Oct 2009). **Image Citation:** [*Cigna et al., 2012*]

DInSAR deformation maps are either displayed in terms of "wrapped" phase or "unwrapped" LoS distance changes. Wrapped phase images display "fringes" that represent LoS deformation as phase change (see Figure 5a), each fringe or 2π colour cycle corresponds to a displacement of

$\lambda/4\pi$ metres, where λ is the wavelength (in metres) of the microwave radar used by satellite. Note that L-Band satellites have a wavelength of approximately 23.6 cm whilst X-band satellites have a wavelength of approximately 3.1 cm (see Table 1 for a list of current and former satellite missions and their specifications). Consequently one fringe of L-band phase change corresponds to 11.8 cm of LoS deformation while one fringe of X-band phase change equates to 1.6 cm of deformation.

The temporal evolution of subsidence for a given location can be obtained when a set of DInSAR images are used in an advanced DInSAR processing. In this case the phase fringes are "unwrapped" to produce maps of absolute LoS displacement over time (see Fig 5b). Unwrapping is the complex process that involves converting wrapped phase DiNSAR images into images of total deformation relative to some reference or reference pixel. Therefore, for every radar measurement, advanced DInSAR provides: (1) the 3 dimensional (3D) geographic position of point measured, (2) the temporal evolution of the LoS displacement over the analysed time period or interferogram stack (Figure 6).

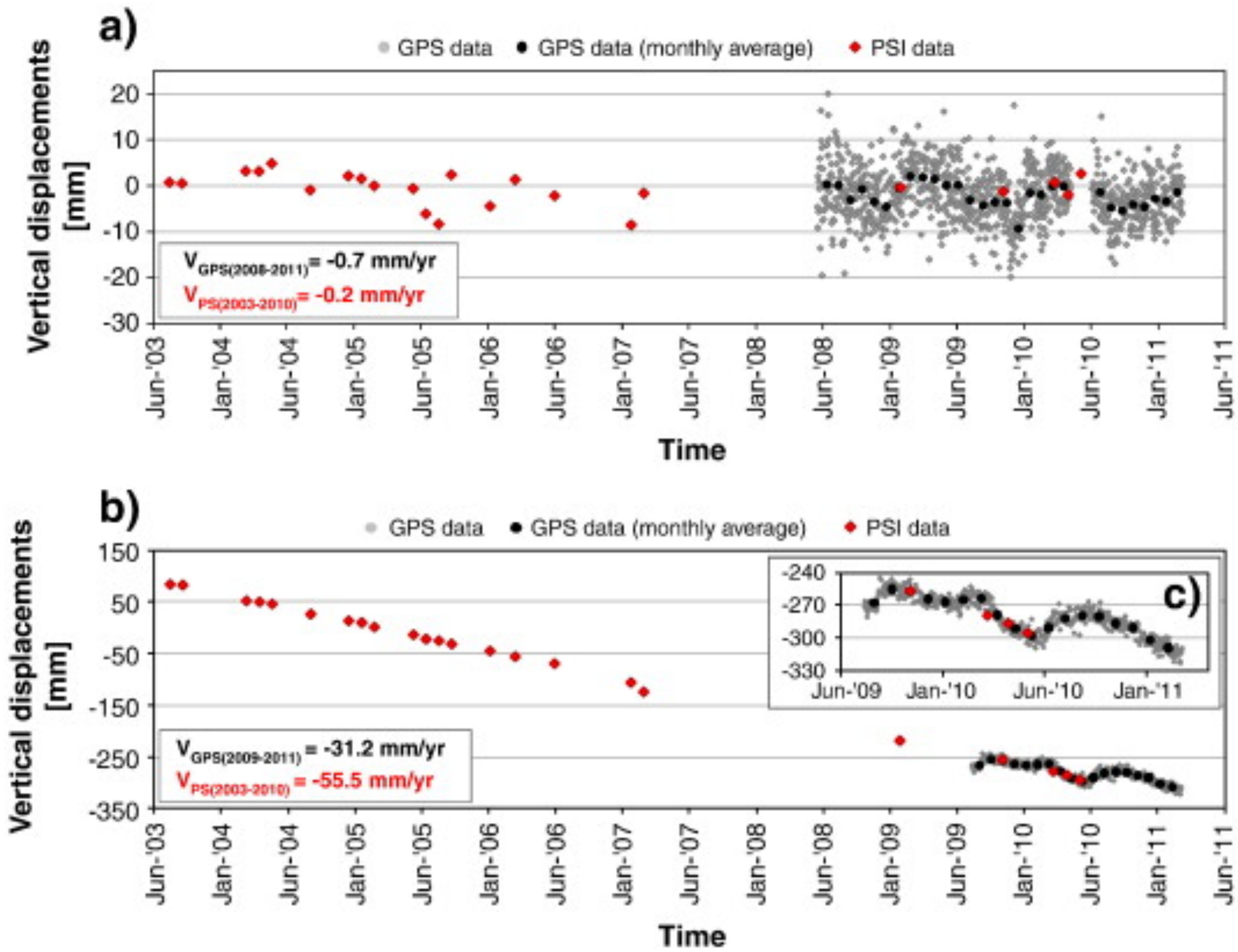

Figure 6. Vertical displacement time series for GPS sites and their respective nearest PS InSAR pixels (i.e. closest radar targets to each station). GPS site MOGA (a), is located just off the bottom right corner of area shown in Figure 5, and MOIT (b) located at position 1 in Figure 5. Magnified view (c) of the overlapping GPS / PS InSAR time series for station MOIT is also shown. **Image Citation:** [*Cigna et al., 2012*].

2.1.2.3 Strengths and weaknesses of InSAR

Strengths

- High spatial resolution of deformation pattern.
- Good measurement precision. InSAR line-of-sight deformation measurements under normal observing conditions have uncertainties of 10 millimetres or less.

- Little or no ground instrumentation required.
- Reasonable temporal sampling resolution of a few days to a few weeks, depending on the particular satellite mission used.

Weaknesses

- Data availability. Radar instruments onboard SAR satellite missions don't always operate continuously. In particular, images are typically acquired when requested by an end user and programmed by the mission manager to do so. Future image requirements for particular CSG monitoring programmes would need to be scheduled in advance.
- Utility of historical data will be governed by the so-called "baseline lengths" between the satellite(s) at the time of acquisition of each image. If either the spatial or temporal baseline distances are too large then the accuracy of the deformation estimates will be degraded. The baseline limitations vary depending on the SAR system used with the longer wavelength L-band observations usually allowing larger baselines than the shorter X-band observations.
- A high-resolution digital elevation model is required in the processing of the image data. Such models are available, but the accuracy would need to be validated in the area of CSG activity.
- High quality knowledge of the atmospheric water vapour content is required in the processing of the images. Otherwise, retardation of the signals as they propagate through the atmosphere will create erroneous ground deformation signals. Information on tropospheric water vapour content can be provided with sufficient accuracy from estimates made by nearby continuous GPS sites or numerical weather models.
- SAR pixel coherence is a necessary requirement for an InSAR ground deformation image to be generated. Coherence refers to the condition when pixels within SAR images appear to have the same surface characterization in all the SAR images used to generate the interferogram.
- The coherence of an interferogram is affected by many factors, including:

  - Topographic slope angle and orientation (steep slopes lead to low coherence)
  - Terrain properties
  - The time between image acquisitions (the longer the time interval the lower the coherence)
  - The distance between the satellite tracks during the first and second acquisitions, also referred to as the baseline (larger baselines lead to lower coherence)
  - Vegetation: Changes from one scene to the next, as plants grow and die are sufficient to change the surface characterization and cause decorrelation. This is a particular problem for X-band and C-band sensors. L-band sensors overcome this limitation in many situations, because their significantly longer wavelength is able to penetrate through foliage and reflect off objects beneath the vegetation.
  - Construction: at a construction site, the appearance of the land surface is changing constantly.
  - Erosion: whether prompted by rain, snowmelt or wind, surface erosion will also change the surface characterization of land and, thereby, can decorrelate those areas where erosion is prevalent.
  - Rapid movement: landslides and earthquakes precipitate rapid motion of an area of land. Quite often, the rapid motion causes destruction and, with it, a total change in the land surface appearance.

Coherence is measured by an index ranging from 1 when an area is completely coherent, to 0 if an area is completely decorrelated. In general, interferometry is successful and accurate deformation is measurable when the coherence index lies between 0.5 and 1.0. Interferometry can still produce meaningful results with coherence levels below 0.5 but, as the index gets lower, the results will display increasing levels of noise and may show erratic deformation patterns from scene to scene, although movement trends remain visible and are generally reliable.

For measuring ground displacement, satellite-based DInSAR techniques present three major advantages compared to other classical ground-based methods, such as GPS:

1. They provide low-cost displacement measurements across wide areas and with a high spatial density, as opposed to the discrete point data obtained from ground based techniques, restricted to discrete benchmarks having with a much lower spatial density. As an example, the widely used SAR images acquired by the European ERS or ENVISAT and the German TerraSAR-X satellites cover an area of 100 km x 100 km and 30 km x 50 km, respectively.
2. Orbital sensors have a short revisiting time period, which makes it possible to monitor subsidence at a relatively high frequency.
3. The low incidence angle of the SAR measurements (i.e. the angle between the satellite line-of-sight and a line perpendicular to the land surface) makes the InSAR technique very sensitive to vertical displacements produced by subsidence.
4. The relatively long archive of SAR images acquired since 1992 potentially allows studying of areas that currently have not been instrumented with ground sensor systems.

Nevertheless, due to the weaknesses discussed above, DInSAR techniques should be considered as complementary, rather than a complete replacement of the ground-based techniques for monitoring subsidence.

2.2 Aerial Monitoring

2.2.1 Airborne LiDAR

Airborne LiDAR[5] terrain mapping produces high-resolution topographic maps of very high accuracy. The unique capabilities of this technique yield more comprehensive and precise topographic information than traditional methods. Airborne laser altimeter data can be used to accurately measure the topography of the ground, even where overlying vegetation is quite dense. The data can also be used to determine the height and density of the overlying vegetation, and to characterize the location, shape, and height of buildings and other man-made structures. Repeat observations provide the information necessary to derive estimates of subsidence.

2.2.1.1 How Airborne LiDAR works?

LiDAR surveying is, in principle, relatively straightforward: the method relies on measuring the distance from an aircraft to the Earth's surface by measuring precisely the round-trip travel time[6] of a pulse of laser light [Ackermann, 1999; Carter et al., 2007; Harding, 2000; Figure 7]. The travel-time is converted into distance from the aircraft to the ground by multiplying by the speed of light. Typical LiDAR transmitters used produce a near-infrared laser pulse that is invisible to the human eye. State-of-the-art advanced LiDAR systems can send out up to 150,000 laser pulses per second [Carter et al., 2007]. By scanning the laser pulses across the ground using a rotating mirror, a dense set of distances to the surface is measured [Figure 7] along a narrow swath under the ground track of the aircraft. This is why airborne LiDAR surveys are often also referred to as Airborne Laser Swath Mapping (ALSM).

[5] LiDAR is the acronym for LIght Detection And Ranging. LiDAR is a remote sensing technology that measures distance by illuminating a target with a laser and analyzing the reflected light.

[6] Round-trip travel-time is defined as the time a laser pulse takes to travel from the aircraft to the ground surface and back to the aircraft.

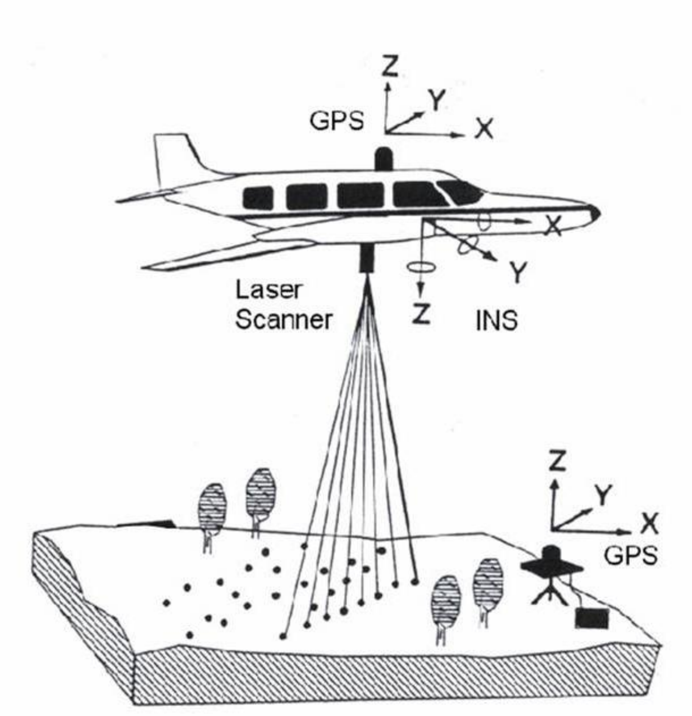

Figure 7. A schematic illustration of an airborne LiDAR system in operation. Adapted from Flood and Gutelius, 1997.

The distance measurements are converted to map coordinates and elevations for each laser pulse by combining the distance data with information on the position of the aircraft at the time the laser pulse was shot and the direction in which the pulse was shot. The aircraft position along its entire flight path is determined from GPS observations using a differential kinematic positioning technique [El-Sheimy et al., 2005, Carter et al., 2007, Shan et al., 2007]. The direction of the laser pulse is established using an Inertial Navigation System (INS) that measures the 3 dimensional (3D) attitude of the airplane, and measurements of the orientation of the LiDAR scan mirror. An area is mapped by flying many parallel lines, guided by GPS, so that the narrow swaths of data overlap along their edges. Perpendicular flight lines may also be flown to produce a grid of observations that can be used to determine and calibrate systematic errors based on comparing measurements at the grid intersections or "crossover" points [Berosa et al., 2007].

The combined set of geo-referenced[7] data points that results from an ALSM survey is often referred to as a "point cloud". Early versions of laser altimeters measured the distance to the first feature reflecting the laser pulse. In areas of dense vegetation that is usually the top of the vegetation canopy. More recent laser altimeter systems measure multiple returns for each laser pulse. Typical modern LiDAR systems produce a laser pulse that has a ground spot size of about 0.5 m in diameter. If the laser pulse reflects off of more than one feature within a ground spot, the one pulse can measure distances to the multiple features. For example, if parts of the laser pulse reflect off tree foliage and branches at several levels and the remainder of the laser pulse reflects off the ground, the elevation of the branches, foliage and ground are represented in the returned pulse waveform. This capability is very important when trying to map ground topography beneath vegetation. The 'last returns' for each pulse are those from the lowest features and thus are more likely to be reflections from the ground. Post-processing algorithms are used to identify the last laser returns that are from the ground. Once the ground returns are identified, they are used to produce what is known as a "bare Earth" digital elevation model (DEM) that describes the ground

[7] "Geo-referenced" data points have coordinates in a reference frame whose origin lies at the centre of the Earth.

topography using a regularly spaced grid of elevation values. In urban areas, a similar separation is done to identify returns from the ground versus those from buildings and structures.

Post-processed LiDAR point clouds are produced in a global reference frame determined by GPS positioning with typical spatial densities > 1 observation per square metre and data point accuracies of up to 3-10 cm in vertical position and 20-50 cm in horizontal position [Glennie, 2007; Toth and Grejner-Brzezinska, 2010; Borsa et al., 2007]. The point cloud observation density recovered depends on the type of LiDAR instrument used and the altitude at which the LiDAR survey is flown. The resulting data products have important applications in many areas. ALSM campaigns have yielded digital representations of topography at resolutions and accuracies sufficient to make measurements of surface deformation associated with earthquakes, landslides, and subsidence associated with ground water depletion. [E.g., Hudnut et al., 2002; Bevis et al., 2005; Oskin et al., 2007, 2010, 2012; Prentice et al., 2009; DeLong et al., 2010; Hilley et al., 2012].

2.2.1.2 Approach to using LiDAR to measure subsidence

To examine motion of the ground surface due to subsidence using airborne LiDAR, geo-referenced bare earth DEM's computed using LiDAR point clouds collected at different epochs can be differenced. The resulting elevation-difference map shows apparent absolute vertical motion of the ground surface in the time interval between the surveys at each DEM grid point. Since the bare earth DEM's can contain a relatively high levels of random noise, often a smoothing filter with a radius window of 1-5 metres is used before the differencing step. This technique of measuring subsidence results in maps of vertical motion with very high spatial resolutions of >1 sample per square metre and absolute vertical accuracies of about 10 cm [Oskin et al., 2012]. This level of accuracy is about an order of magnitude worse than can be obtained using either GPS or InSAR measurements, and thus would only a useful technique form monitoring areas where subsidence rates exceed at least several cm per year.

2.2.1.3 Strengths and weaknesses of the approach

Strengths:

- High-density maps of deformation >1 sample per square metre.
- LiDAR surveys can be scheduled and flown any time (within weather limitations).
- Can make measurements in all terrain and vegetation conditions.

Weaknesses:

- Accuracy is only 5 - 10 cm in the vertical component.
- Specialized processing of data is required to obtain the highest accuracy results, which may not be available from commercial operators.
- Surveys can only be flown in good weather.

2.2.2 Airborne InSAR

Over the last three decades, differential SAR interferometry (DInSAR, see Section 2.1.2.1) has proven to be a valuable technique for measuring both naturally occurring and anthropogenically induced deformation. Until relatively recently, most DInSAR observations have been made using space-borne systems that have repeat intervals of weeks to months or greater and produce deformation fields with spatial resolutions of 25 metres or more. Using advanced DInSAR processing techniques described in Section 2.1.2.2, these sensors have been used to monitor deformation across an array of both natural and man-made structures including large scale structures such as dams, hydrocarbon reservoirs, and mines [Tarchi et al., 1999, D. Perissin et al., 2009, Van der Kooij and D. Mayer, 2002, Ng et al., 2010]. Using the same technology and processing algorithms, an appropriately configured airborne SAR sensor can theoretically make similar measurements while removing many of the limitations found in space-borne observation (scheduling of image acquisition, dependence on international satellite missions for data, etc.). The flexibility to schedule observations and to fly airborne SAR sensors with the most appropriate geometry for a particular application makes airborne SAR arguably a more robust monitoring platform. The main problems in translating DInSAR deformation observations from space-borne to airborne systems is in characterising the irregular flight trajectories flown by aircraft systems and the variation in the aircraft attitude angles from pass to pass when compared to the more stable space-borne flight trajectories.

2.2.2.1 How airborne SAR works

The development of airborne SAR radar systems sometimes referred to as AirSAR or UAVSAR designed specifically for repeat-pass SAR observations and InSAR applications began in about 2003 [Hensley et al., 2005; Chapman et al., 2011]. The airborne SAR technique and DInSAR data processing algorithms used to process the airborne SAR data are, for the most part, analogous to the space-borne methods discussed in Section 2.1.2. Making robust repeat-pass SAR measurements suitable for use in DInSAR analysis of both natural and man made deformation from an airborne platform does however presents some difficulties that are not found in space-borne observations due to the above mentioned navigation and sensor attitude constraints. Key measurements the system has been designed to make include; precision crustal deformation for monitoring earthquakes both during and after a seismic event, monitoring volcanic activity and for monitoring human-induced surface change such as subsidence induced by oil or water withdrawal, or other displacements of the surface from human activities [Hensley et al., 2005].

The first requirement to enable airborne DInSAR to produce deformation measurments is that the aircraft flight track must have a repeatability of <10 metres. This flight precision tolerance is only possible on suitable modified aircraft with precision autopilot capability [Lee et al., 2007]. The precision autopilot uses input from the real-time differential GPS to generate signals that are used to precisely navigate the aircraft. State of the art precision autopilot systems have been shown to exceed this requirements and can typically fly aircraft along repeat flight paths with better than 5 m accuracy [Lee et al., 2007]. The second important prerequisite to enable coherent DInSAR images to be formed is that repeat antenna look directions are identical to within a fraction of the SAR beam-width. Because the winds aloft can be substantially different at different flight times, even if the platform is capable of accurately repeating the desired track, the yaw angle (or pointing attitude) of the aircraft can vary widely on different passes due to variable wind conditions. To overcome this problem, Airborne SAR systems must be able to either able to electronically steer the SAR antenna to the desired direction based on real-time aircraft attitude angle measurements, or use motion compensation algorithms in the data processing to account for this SAR antenna motion and mis-pointing error.

2.2.2.2 Approach to using airborne SAR to measure subsidence

AirSAR is a very accurate and flexible method for monitoring ground subsidence. Because the instrument mounted on an aircraft, the timing and geometry of SAR surveys can be configured to acquire data at the most appropriate temporal and spatial resolutions. Figure 9 shows a DInSAR image from 2 NASA UAVSAR flights over Lost Hills, CA on May 6 and July 25 of 2008. The images were collected from an altitude of 12.5 km. This area is known to be undergoing surface deformation due to oil pumping based on satellite radar interferometric measurements and GPS measurements. The space-based InSAR subsidence maps are show in Section 2.1.2.1, Figure 4.

The area is mostly agricultural interspersed with light urban development and thus many areas remain highly correlated for large temporal baselines at L-band. Obvious from the radar interferogram are two areas undergoing surface deformation centered over light urban areas. Figure 9 shows the “line-of-sight” displacement obtained and has a spatial resolution of about 7 m. L-band has good correlation over the urban development and in some fallow agricultural regions. The maximal displacement is about 7 cm corresponding to a deformation rate of about 1.0 mm per day.

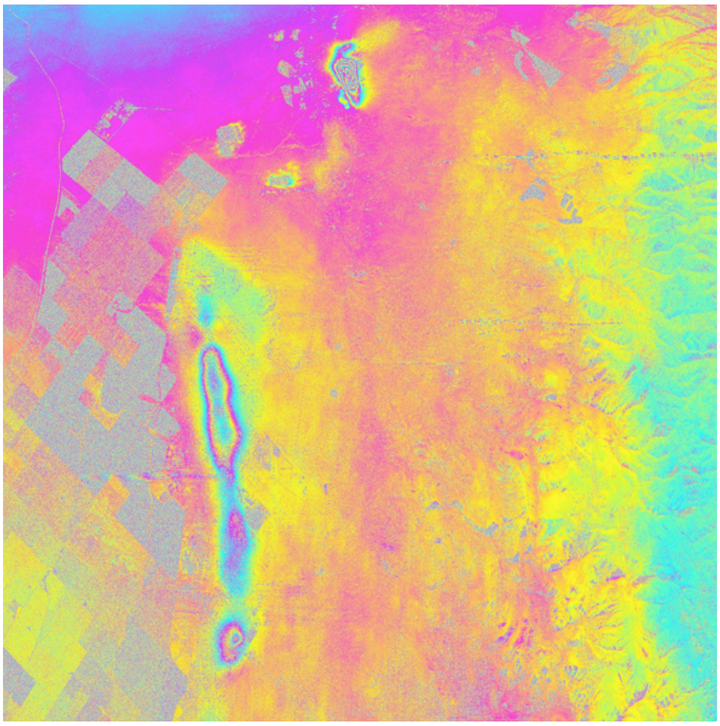

Figure 9. UAVSAR wrapped UAVSAR DInSAR image of the Lost Hills oil field in California USA. **Image Credit:** NASA/JPL.

2.2.2.3 Strengths and weaknesses of the Airborne InSAR approach

Strengths:

- Observations can be scheduled at any time unlike space-based InSAR where the satellite returns period is fixed and depends on orbital configuration.
- Observations can be collected from different look directions and angles enabling a full 3D deformation field to be estimated. Spaced based InSAR observations in general do not allow monitoring ground deformation components in North-South direction due to the above orbital limitations.
- Higher spatial and temporal resolution imaging is possible than from a space-based platform.

Weakness:

- The cost of building, maintaining and operating a dedicated SAR aircraft platform is very high.
- Though very promising for precise monitoring of ground subsidence, present AirSAR systems are currently still in the R&D phase of development and therefore not yet commercially available.

2.3 *Land-based Monitoring (terrestrial techniques)*

There are a number of land-based measurement systems that have traditionally been used by surveyors to monitor and quantify land surface deformation, including levelling and a combination of high precision angle and electronic distance measurement. These techniques are still viable and can still deliver subsidence estimates accurate to ~10 mm; however, they are labour-intensive and best suited to small regions only.

2.3.1 Optical Levelling

Optical levelling is a traditional surveying technique for determining the elevations of points on the Earth's surface relative to some starting point or height datum. Surveyors place points or monuments, referred to as "benchmarks", in or on the ground, and make repeat measurements over a period of time to measure changes in height. It is not possible using this technique to measure changes in horizontal position. There are several different leveling techniques surveyors can use to determine the relative heights of benchmarks, and the method selected depends on the scale of the field area over which height information is required, the type of terrain to be levelled, and the accuracy with which of the height measurements are needed determines the method that will be adopted.

2.3.1.1 How does Optical Leveling work?

The instrument used for optical leveling is known as an optical level. Generally mounted on a tripod, the optical level enables the observer to sight along a horizontal line, that is a line perpendicular to the local gravity vector. By reading the height of benchmarks below this horizontal line using a precise ruler commonly known as a "staff", the relative heights of different benchmarks can be determined. By repeating this process in a leapfrog manner and adding up all the differences in height, the total difference in height between two distant points can be calculated. If the first point is a tide gauge or a benchmark where Mean Sea Level height has been previously established, then all the points measured in the survey will have known heights above Mean Sea Level.

Over long distances optical leveling is a time consuming and laborious technique, but produces relatively accurate results. Depending on the instrument used and the care taken by the surveyor, typically achievable optical levelling the accuracy is; 8mm x √(distance in kilometres) which equates to about 25mm over 10km, or 80mm over 100km.

2.3.1.2 Strengths and weaknesses of the approach

Strengths

- Straight-forward and direct approach to measuring changes in height
- Can be very accurate over short distances (up to a few km)

Weaknesses

- Very time consuming and labour intensive
- Not appropriate for broad-scale ground deformation. Being a relative measurement technique, at least some of the levelling benchmarks must be placed outside the deformation zone in order to quantify the total deformation that is occurring.

2.3.2 EDM Height traversing

Through the application of simple trigonometry, the change in height between two points can be deduced from the angle of elevation of a line joining two points and the distance between them. Using this principle, the technique of "EDM height traversing" can also be used to determine changes in height (and also horizontal position). The technique has similar strengths and weaknesses as optical levelling and will not be discussed in further detail.

2.3.3 Terrestrial LiDAR or Terrestrial Laser Scanning (TLS)

Terrestrial LiDAR (T-LiDAR) or Terrestrial Laser Scanning (TLS) use much the same technology and processing algorithms discussed in the airborne LiDAR section (2.2.1). Rather than being mounted on an airborne platform however, TLS instruments are mounted on tripods on the ground. TLS systems are setup and operated from various user-selected positions, ensuring complete shadow-less scan coverage of the feature of interest. Reflective targets with known geographic coordinates may be placed around the feature and are used to facilitate alignment of the final point cloud and place it in a global reference frame. During a TLS survey, the scanner makes measurements from various aspects at ranges of 100 m – 5 km from the target area. Shot densities for typical TLS point clouds can be > 10,000 per square meter and the variable aspect acquisition geometry enable a true three-dimensional (3D) representation of the scanned target (Figure 10). In addition, TLS systems also typically employ high-resolution digital colour photography so that red-green-blue (RGB) values acquired by a TLS digital camera can be used to colour the point clouds and produce photorealistic images.

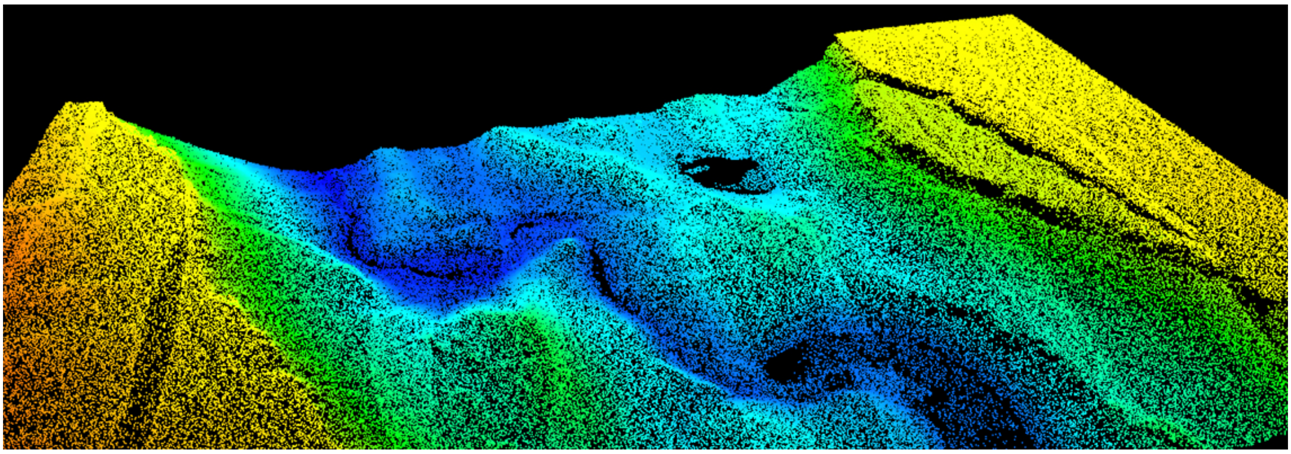

Figure 10. TLS LiDAR point cloud from a landslide area near Salmon Falls, Idaho, USA. **Image Credit:** Idaho LiDAR Consortium

2.3.3.1 How does terrestrial LiDAR or TLS work?

TLS instruments work by emitting light (usually in the near infra-red wavelength) and detecting the reflected light in order to accurately determine the distance to the reflected object. Rather than making a single measurement as in a laser rangefinder, TLS systems have rotating mirrors that allow millions of measurements to be made over a scene in just a few seconds or minutes (depending on the type of scanner). There are two primary types of 3D laser scanners: time-of-flight scanners and phase-shift scanners. Time-of-flight laser scanners emit pulses of laser light that are reflected off the scanned object. The sensor measures the time of flight for the optical pulses to travel to and from the reflected surface. As with airborne LiDAR systems, TLS have the ability to measure several arrival times for an emitted pulse. So, for a scan of an area with vegetation, the "first arrival" would indicate the distance to the top of the vegetation, and the "last arrival" would indicate the distance to the ground surface or "bare earth". For phase-shift TLS systems[8], the reflected light received is compared with emitted light to determine the phase shift. This provides a precise but ambiguous measurement of absolute range. Multiple modulation frequencies are used to convert the precise phase shifts measurements into absolute ranges to the target.

[8] Phase shifting TLS systems use a laser beam with sinusoidally modulated optical power.

In general the difference between the two types of instruments is that "time of flight" scanners have the ability to measure targets at longer ranges while phase shift scanners can sample and scan areas more quickly and produce higher resolution images.

TLS instruments emit thousands of pulses per second at different known azimuths and elevations using a rotating mirror system, thus generating distance values for millions of points that reflected the light. Using the known position of the TLS instrument sensor and the distance and the orientation that the laser pulses were fired, the coordinates associated with each reflected pulse can be determined. In addition, the intensity of the returned pulse is also measured. The combined coordinates and associated intensity values for millions of data points measured make up the target area "point cloud".

TLS accuracy is affected by both systematic and random errors. Systematic errors are governed by range error and angular error[9]. Systematic errors translate to a typical accuracy of about +/- 25 mm at 1000 m. Random errors in general relate to the incidence angle of the laser pulses on the target, as well as the reflectivity properties of the target. Random errors affect the precision of the measurement, which is variable, but generally between 0 – 10 mm, regardless of distance. Pixel resolution of TLS equipment is based on the distance between the target and the scanner due to beam divergence therefore the pixel spacing in the point cloud and the sampling resolution varies for every target area surveyed.

2.3.3.2 Approach to using terrestrial LiDAR to measure subsidence

In a typical TLS survey the number of individual scans of the target area varies according to the scale and complexity of the site, but a typical survey consists of 5-10 scans, collected from various aspects, that are "stitched" together to form a single point cloud. The resulting point clouds are then used to produce either DEMs or solid-surface models. The accurate digital 3D models of the ground surfaces from repeating surveys of the same locations at regular intervals enables analyses of changes in space and time to be undertaken. The methods for estimating deformation of ground subsidence from TLS measurements are based on point cloud matching using algorithms for Least Square 3D Surface Matching proposed by Gruen and Akca [2005]. Or more a recent approach described by Monserrat and Crosetto [2008], which takes advantage of both surface matching and curve matching to improve quality. Both methods exploit the high density of TLS point clouds to offset the relatively low precision of individual TLS points. Terrestrial LiDAR has been used for a variety of applications such as the monitoring of; volcanoes [Hunter et al., 2003; Jones, 2006], earthquake and mining subsidence, [Hiatt, 2002] and landslide deformation [Rowlands et al., 2003; Hobbs et al., 2002].

In general TLS for monitoring ground deformation is only suitable for surveying relatively small target areas on the scale of 1 – 10 square kilometres. In addition the technique requires the scanner be able to view the target area from multiple locations, and that the scanner is located outside the deformation area itself. Therefore for the scales and gradients of deformation that might be expected from CSG activities at depth this technique is probably suitable in most instances.

2.3.3.3 Strengths and weaknesses of terrestrial LiDAR

Strengths:

- Produce very high-resolution images.
- Produce very accurate 3D DEMs.

[9] Range error is error in the measurement of distance between the scanner and the target. Angular error is the error in the positioning of the scanners rotating mirrors.

- Provides a flexible data collection and processing system.
- Surveys a quick to complete and relatively inexpensive.
- TLS is a commercially available technology.

Weaknesses:

- TLS surveys sample relatively small apertures of 1 – 10 square kilometres.
- TLS is only useful for monitoring very localized deformation and subsidence processes.
- Requires experienced surveyor who understands the limitations of TLS systems.
- Requires a well-designed data collection strategy to avoid shadowed regions and optimise 3D accuracy of processed DEMs.

2.3.4 Terrestrial or Ground-Based InSAR

Terrestrial or Ground-based interferometric synthetic aperture radar (T-InSAR, GB-InSAR) uses radar waves to map ground movement. The technique is fundamentally similar to space-borne and airborne InSAR methods discussed in Sections (2.1.2) and (2.2.2) but instead of acquiring the images from several kilometres to several hundred kilometres away, the images are acquired by a radar moving along a rail within a couple of kilometres of the area of interest. While the space-based and airborne system collects images every few days to weeks, the ground-based system is capable of acquiring images as often as every five minutes. This allows almost continuous monitoring of movement ranging from millimetres per year to metres per hour in velocity. The working target range of ground based InSAR systems is up to four kilometres in line-of-site distance.

2.3.4.1 How does terrestrial InSAR work?

T-InSAR is a radar technique for remotely monitoring displacements of the ground surface within the target area. By precisely moving a radar sensor along a linear rail, two-dimensional (2D) SAR images can be derived. By comparing the phase difference (using the interferometric SAR technique described in Section 2.1.2) of each pixel between two or more SAR images acquired at different times, the displacements along the instrument line-of-sight are derived. Thus, 2D images of line-of-sight displacement can be achieved as well as the displacement time series of each pixel (Figure 11). Continuous T-InSAR monitoring can be achieved by permanently installing the equipment at a stable location that overlooks the target area. The equipment can be programmed to collect data at regular intervals defined by the user. The technique does not require the installation of other sensors or reflectors in the target area.

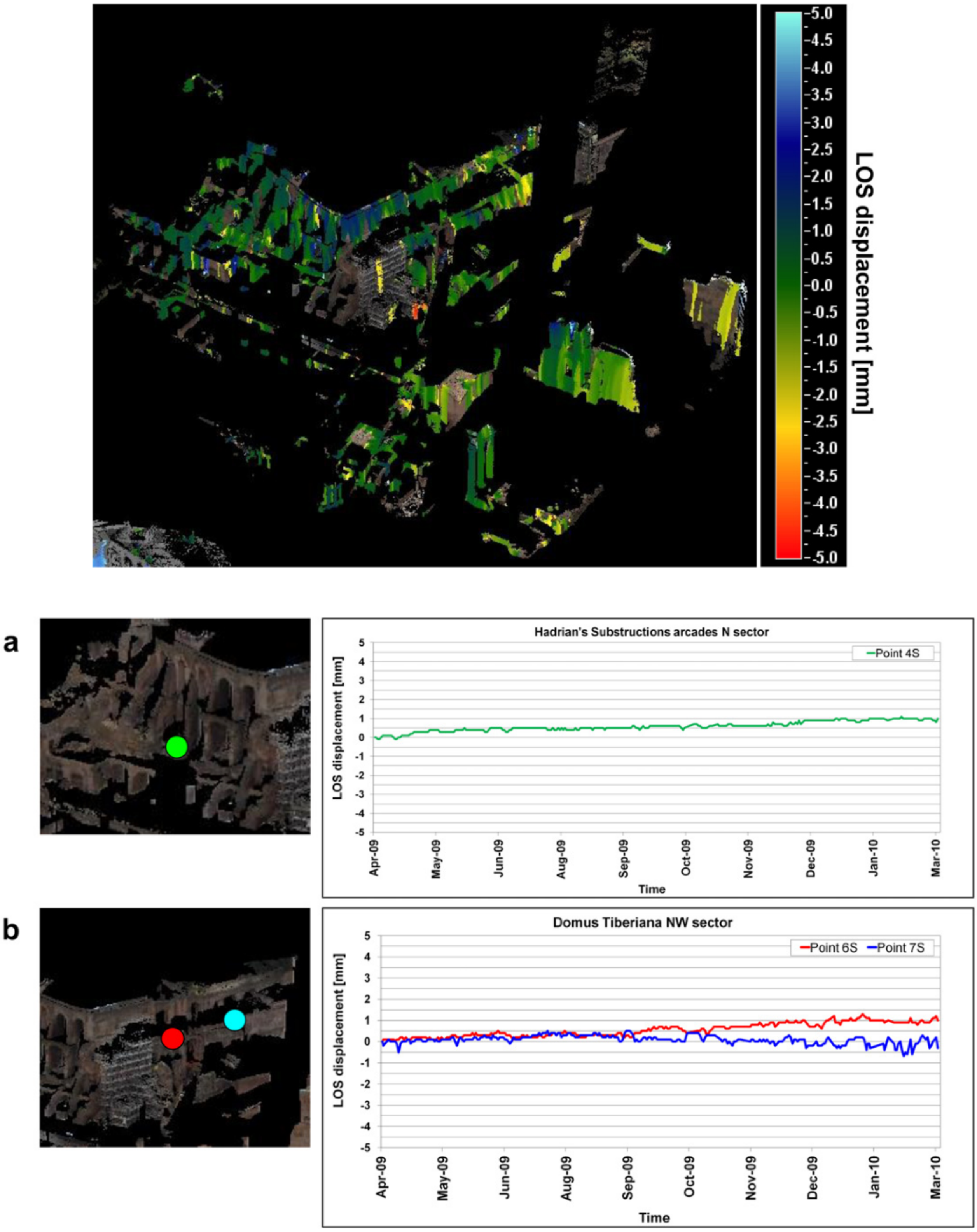

Figure 11. Top) 3D image of the Domus Tiberianaa near Rome, Italy, draped with T-InSAR cumulative line-of-sight displacements measured over the period April 2009 - March 2010. The structure was continuously monitored while archaeological excavations were being performed. **Bottom)** T-InSAR time-series of locations indicated by coloured dots showing the high temporal resolution and very high precision achievable with the T-InSAR technique.

2.3.4.2 Approach to using terrestrial InSAR to measure subsidence

The theoretical accuracy of T-InSAR systems is on the order of ±0.1 mm. However, both the precision and the accuracy are strongly influenced by the atmospheric disturbances as discussed in Section 2.1.2.3. In practice, the precision of the technique ranges from ±0.1 mm to ±3 mm, depending on the monitoring distance and the atmospheric conditions. The pixel resolution of a terrestrial SAR image ranges from few decimetres to several metres (depending, again, on the equipment and on the monitoring distance). At a distance of 1 km, the most common commercial available equipment has a resolution of about 0.5 - 4 m.

The best application of T-InSAR is the continuous monitoring of unstable slopes and dams. Other applications include linear infrastructures such as bridges, very localized subsidence and buildings where the instrument can illuminate the target with radar signals at high incidence angles. TInSAR monitoring of broad-scale subsidence will, in most instances, be quite challenging because, although it is possible to collect highly accurate sub-mm 2D displacements, the low incidence angle of radar illumination will mean the interferometric measurements will be relatively insensitive to any vertical movements that are associated with subsidence.

2.3.4.3 Strengths and weaknesses of terrestrial InSAR

Strengths

- Ability to very precisely monitor 2D displacements very precisely from a remote position, without the installation of targets or sensors.
- Ability to measure continuously, day and night in any weather conditions, including rainfalls, clouds and fog.
- Can achieve high target area sampling rates of every few minutes
- Provides relatively high spatial density of observations.

Weaknesses

- The size of commercial equipment (up to 3 metres long).
- Very limited field of view (some tenths of degrees in both the horizontal and vertical planes.
- Can only measure displacement along the instrument line-of-sight.
- There is the possibility of signal phase ambiguity for large deformation (i.e. displacement higher than 5 mm between two consequent images).
- Short range < 5 km.
- Single fixed look direction means shadowing is problematic.
- Only works well for monitoring vertical deformation in situations where there is substantial vertical relief available.

2.4 Other techniques

2.4.1 Tilt Meters

Tilt meters measure temporal changes in slope and, with precisions as small as 1 nanoradian (~0.0002 arcseconds), they can provide one of the most precise measurements of ground movement. Arrays of tiltmeters are well suited to providing long-term, continuous monitoring of subsidence or uplift caused by removal or injection of gas/fluids.

2.4.1.1 How do tiltmeters work?

A tiltmeter measures the gradient of surface movement. Simplistically, a tilt meter is a sophisticated spirit level, containing a fluid-filled tube with a bubble. As the instrument tilts, the bubble moves within the tube to remain aligned with the local gravity vector. The movement is measured and converted into an estimate of the tilt of the instrument. The measured changes in tilt must be integrated to derive estimates of surface displacement, and there are many case studies that document the effectiveness of this approach [e.g. Davis et al., 2008].

2.4.1.2 Strengths and weaknesses of tilt meters

Strengths

- Highly precise measurements. 1 nanoradian tilt of a line between Sydney and Perth is equivalent to a height change of ~4 mm.
- The highly precise measurements of tilt allow for variations in subterranean gas/fluid reservoirs to be estimated, providing potentially useful information on the CSG activity being undertaken.

Weaknesses

- Tiltmeters do not measure surface subsidence directly; rather, the tilts must be integrated to derive surface movement.
- Tiltmeters do drift with time. Thus, while the instantaneous precision can be as small as 1 nanoradian, some calibration of the instruments is required in order to maintain accuracy at this level.
- Tiltmeters are relatively expensive. A network of ~40 tiltmeters to monitor a 500 x 500 m region would cost around $36,000/month[10]

2.4.2 Gravity

Changes in subterranean masses (e.g. extraction or insertion of water or gas) will cause observable changes in surface gravity, through both the direct attraction effect and through the gravitational change caused by the associated uplift or subsidence. While observations of either surface or airborne gravity could be used to quantify the mass changes, this approach is likely to be expensive and is not likely to yield information that is superior to methods described above.

Space gravity missions (e.g. GRACE[11]) detect temporal changes in mass distribution on Earth and have been used in Australia to detect groundwater variations [Leblanc et al., 2009], surface hydrology [Awange et al., 2010] and surface deformation [Tregoning et al., 2009]. However, the spatial resolution is limited to ~300-400 km, making this an unviable observing tool for detecting subsidence related to CSG activities.

---

[10] An approximate cost was provided by Halliburton Pty. Ltd. for their Pinnacle system. We do not endorse their system; rather, we present the value as being indicative of what is currently available from commercial operators.

[11] The Gravity Recovery and Climate Experiment (GRACE) is a joint NASA/DLR space gravity mission that was launched in 2002.

3. Measurement of baselines

The measurement of a baseline refers to data that may be collected or observations made before CSG activities commence in a particular location. This then allows changes detected through subsequent measurements to be used to identify the ground deformation caused by the CSG activity.

In the case of using GPS to measure subsidence, simply installing the equipment at any time before the CSG activities commence will enable baseline measurements against which subsequent subsidence can be compared. However, detecting sub-cm subsidence against baseline measurements would require at least 6 months of GPS observations prior to the commencement of CSG activities, so that the background noise inherent in the measurements could be reduced through an averaging process.

A LiDAR baseline measurement would involve undertaking at least one airborne survey prior to the commencement of CSG activities. Such surveys are typically completed in a matter of days, although scheduling the survey with available commercial companies may involve a lead-time of several weeks. There would be some improvement in the accuracy of the baseline measurement, and hence in the subsequent subsidence estimates, by conducting more than one pre-activity LiDAR survey, since the surface elevations estimated in each survey could be averaged thus generating a mean surface elevation model that would have less error than the results of each individual survey. However, the cost of the baseline measurements would increase.

The technique with the most problematic baseline measurement scenario is InSAR, and the problem relates to the current lack of operational SAR satellite missions. The process of estimating deformation from InSAR requires a temporal continuity of images so that the coherence between images can be maintained. Too great a time period between images (i.e. around 12 months) tends to result in too many changes on the ground surface, making it virtually impossible to relate one image to the other. This causes a break in the time series of deformation.

There is potential to make use of existing SAR images over CSG activity areas in order to generate baseline measurements. However, estimating ground deformation relative to such baseline measurements will require the provision of temporal coherence between existing and future images. Given the currently limited supply of images from functioning SAR missions, this is problematic. Table 1 provides a list of the past, current and future SAR satellite missions.

Table 1. Past, current and future SAR missions

Mission	Agency	Band	Launch Date	End of Mission
ERS1	ESA	C	17-Jul-1991	10-Mar-2000
ERS2	ESA	C	21-Apr-1995	05-Sep-2011
Envisat	ESA	C	01-Mar-2002	09-May-2012
ALOS	JAXA	L	24-Jan-2006	12-May-2011
COSMO-1	ASI	X	08-Jun-2007	-
TerraSAR	DLR	X	15-Jun-2007	-
COSMO-2	ASI	X	09-Dec-2007	-
COSMO-3	ASI	X	23-Oct-2008	-
TanDEM-X	DLR	X	21-Jun-2010	-
COSMO-4	ASI	X	05-Nov-2010	-
ALOS 2	JAXA	L	Dec-2013	-
Sentinel 1	ESA	C	Oct-Dec 2013	

An alternative approach to establishing baseline InSAR measurements is to schedule and acquire new images now, before the commencement of CSG activities. Unfortunately, the only SAR missions currently operating operate in the X-band, which provides the lowest spatial resolution, and cannot be combined subsequently with higher resolution images from the future missions of ALOS 2 and Sentinel-1. Therefore, it will not be possible to make InSAR baseline measurements until ALOS 2 and/or Sentinel-1 are launched in the latter part of 2013.

A possible hybrid approach could be to use existing C- or L-band SAR images to obtain a measure of the background level of stability of the region. Then, when new satellite missions are functioning, commence an observing programme and compute the deformation relative to the first available image of the new mission. The use of InSAR imagery in this manner will not quantify any deformation that may occur between the start of CSG activities and the first image acquired by the new mission; however, a bridge between baseline measurements using existing InSAR images and the new missions could be provided through either repeat LiDAR surveys or through the installation of continuous GPS sites. These latter two observations would quantify in an absolute sense any deformation that may occur between the two different sets of InSAR imagery.

Table 2. Comparison of techniques for measuring subsidence

	GPS	**InSAR**	**Airborne LiDAR**	**Terrestrial LiDAR**
Sample Density	1-100 sites/10 km^2	10,000 pixels/km^2	1-10 hits/m^2	1000 hits/m^2
Position Precision	1-20 mm	2-3 m	15-25 cm	1-5 cm
Subsidence Detection	1-5 mm	1-2 cm	10 cm	1 cm
Scale	Global	100 km	10-100 km	1 km

4. Existing recording/measurement of subsidence in areas associated with CSG production

We have not identified in the peer-reviewed scientific literature any published studies related to subsidence associated with CSG production. However, there are many studies that document observed subsidence associated with both injection and production of hydrocarbon and water resources and many of these have been used throughout this report as examples in the technique description sections. CSG processes involve extracting gas and injecting/extracting ground water, so it is reasonable to infer that subsidence deformation associated with such activities in other mining operations will be a good proxy for what might be expected in terms of subsidence detection from CSG activities.

The most common scenarios from subsidence monitoring programmes in general do not rely on any single measurement technique, but apply a combination of different observing techniques. The reason a combination of techniques are often used is that; a) as discussed above many of the techniques proved complimentary information at different precisions and accuracies on the spatial and/or temporal patterns of subsidence deformation, and b) the combination of techniques enable cross validation of results and calibration of the uncertainties of the various measurements used. Below we provide details of some examples where a combination of geodetic techniques has been used to monitor anthropogenic subsidence.

4.1 Tiltmeter and GPS

The combination of tiltmeters and continuous GPS monitoring can provide a monitoring system with high temporal resolution and relatively good spatial resolution over small (500 x 500 m) regions. The tiltmeters provide highly precise measurements that can be integrated to yield surface movement, while a sparse GPS network over the same region can provide the long-term surface movement that calibrates the drift of the tiltmeters. The combined system overcomes the spatial limitation of GPS alone and the potential problem of drift of the tiltmeters.

Davis et al [2008] showed an example of using 44 tiltmeters over a 250,000 m^2 area to detect subsidence of ~200 mm caused by the migration of steam to the surface. Ground-truth observations showed that the tiltmeter-only solution was in error by several tens of millimetres because of the drift of the tiltmeters over a 12-month period. The assimilation of position changes from only 4 GPS sites within the region removed the tiltmeter drift errors and provided a spatially dense estimate of deformation that was thought to be significantly more accurate [Davis et al., 2008].

4.2 GPS and InSAR

The combination of SAR and GPS observations has been used in numerous studies of subsidence over the last decade [Ng et al., 2010; Cigna et al., 2012; Tomas et al., 2013]. The two techniques offer complementary observations that when combined can provide a complete and accurate measurement of ground subsidence. The GPS technique provides very precise measurements of 3D position (± 2 - 5mm) at a very high temporal resolution (every 1 -24 hours) at discrete locations, while the DInSAR technique provides precise line of sight measurements (±5- 10 mm) every 5 – 30 days at very high spatial resolutions (ground spacing of 5 – 100 metres). While DInSAR alone is often sufficient to identify areas of subsidence, the absolute 3D position and atmospheric delay information provided by GPS enables a more precise quantification of subsidence. The GPS observations also enable the line-of-sight deformation identified by DInSAR to be decomposed into its 3D (horizontal and vertical components) in a rigorous manner. To illustrate the synergies between the GPS and InSAR Figures 12 and 13 show the comparison of DInSAR and GPS derived subsidence resulting from a longwall coal mining operation at the West Cliff colliery in NSW between June 2007 and February 2008. Figure 12 clearly shows the ability of DInSAR to map the gross magnitude and spatial extent of subsidence, while Figure 13 illustrates the ability of the GPS techniques ability to monitor in exquisite detail the precise magnitude and temporal evolution of the subsidence as mining progressed along the coalface. By combining the two observation types, Ng et al., [2010] were able to improve engineering models of predicted deformation for subsequent mining operations in the area.

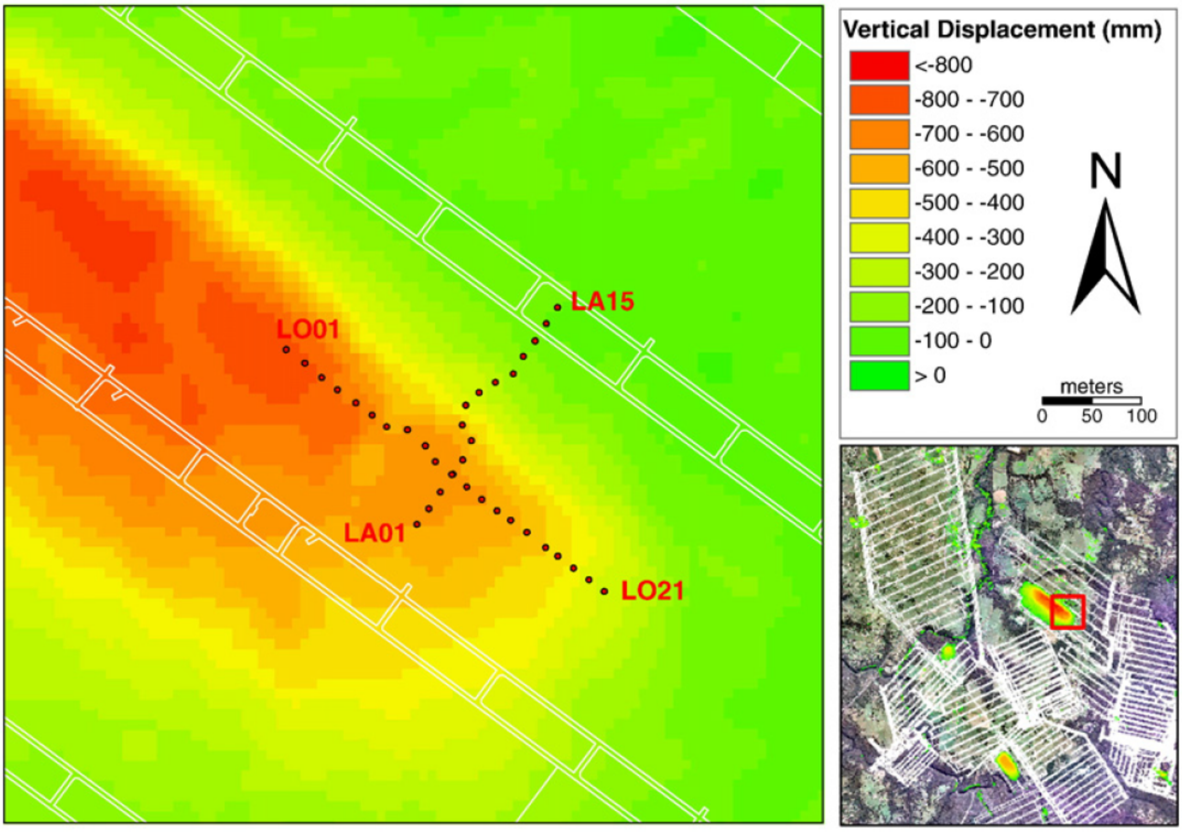

Figure 12. GPS survey points (red dots) overlaid on DInSAR accumulated subsidence map from 29 June 2007 to 14 February 2008, West Cliff Colliery. Negative displacement indicates subsidence. **Image Credit:** [Ng et al., 2010].

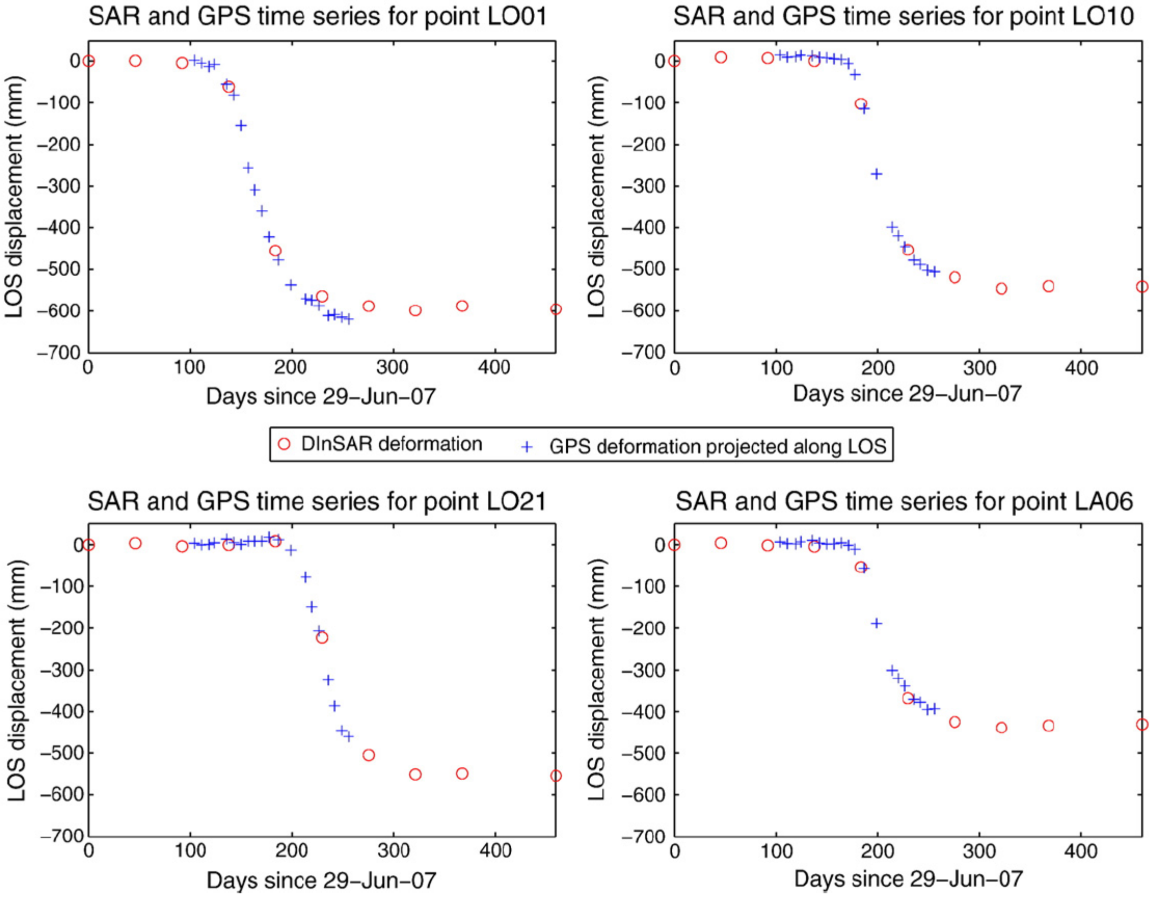

Figure 13. Comparison between DInSAR-measured deformation and GPS-measured deformation time series in days since 29 June 2007 projected along the ALOS-POLSAR "line-of-sight" vector for points LO01, LO10, LO21 and LA06 in Figure 12. The red circles represent the DInSAR measurements and blue plus signs the GPS measurements. **Image Credit:** [Ng et al., 2010].

5. Availability of data online for subsidence in NSW regions with CSG activities

5.1 GPS

Figure 14 shows the current continuous GPS network across New South Wales (CORSnet-NSW) operated by the Land and Property Information (LPI) division of the NSW Government. The data are publicly available but at a cost. Some of the network sites lie in regions with CSG activities and may, therefore, be useful for monitoring subsidence. However, only a few sites lie with 1-3 km of a CSG drill site[12]. The greatest utility of the LPI CORSnet-NSW data will be to augment the regional network of GPS sites, for it is unlikely that the CORSnet-NSW sites will lie sufficiently close to an anticipated subsidence region such that deformation could be detected using CORSnet-NSW data alone.

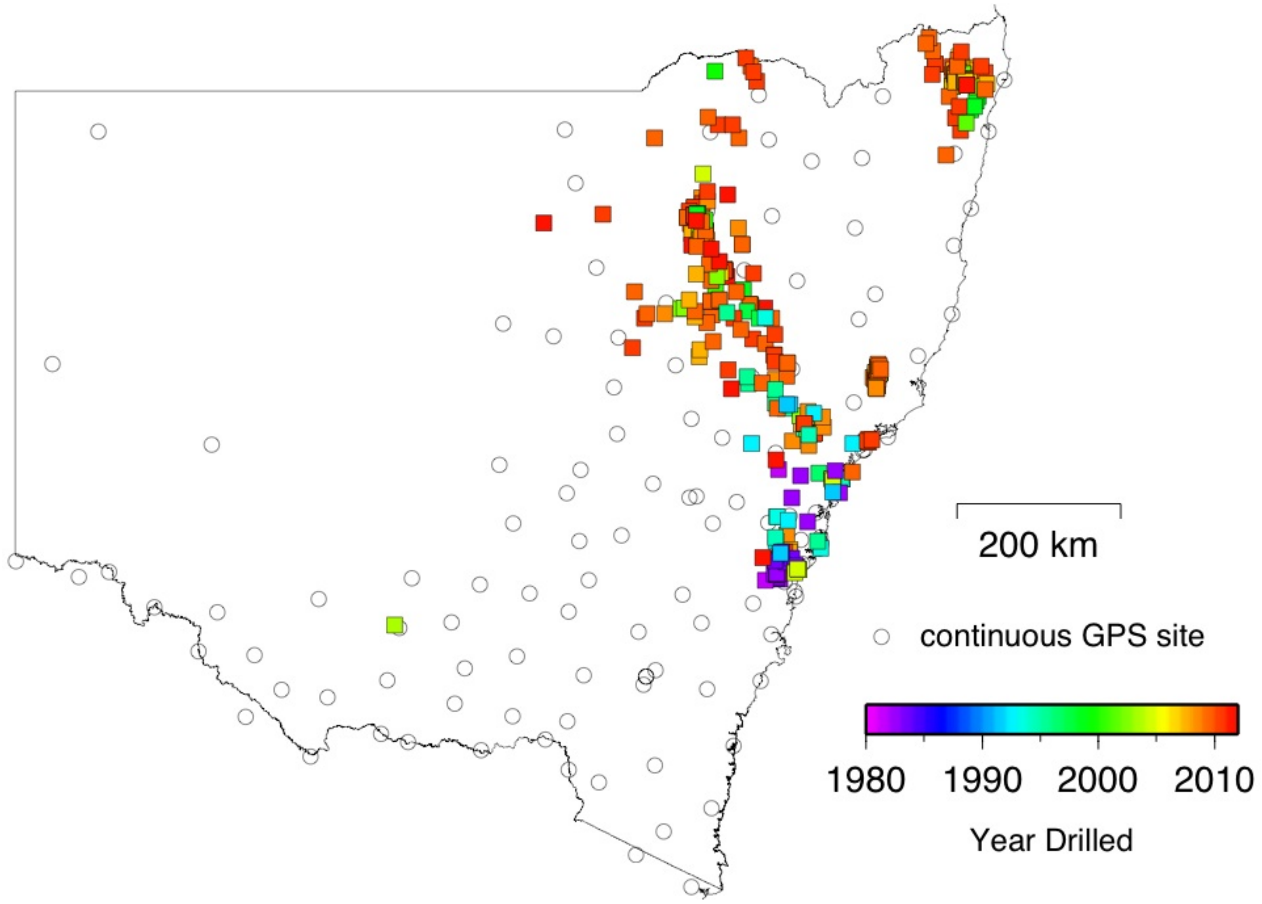

Figure 14. Location of CORSnet-NSW GPS sites shown as open circles (as at 7 June 2013). See http://www.lpi.nsw.gov.au/surveying/corsnet-nsw.
CSG drill hole locations plotted, colour-coded according to the date that the wells were drilled.

5.2 Space-borne InSAR

As outlined in Section 2.1.2, deriving deformation estimates from InSAR requires the continuity of coherence between images so that the interferograms can be formed. This mandates that the temporal separation between the times of acquisition of images is not too long; otherwise changes in land surface coverage alone can cause decorrelation of the images. Additionally, there is no currently operating L- or C-band satellite SAR mission. Consequently, it is unlikely that the

[12] CSG locations for past, current and proposed drill sites provided by NSW Chief Scientist office.

available SAR imagery across NSW will be able to be used as baseline measurements for any future InSAR studies.

On the other hand, SAR images exist across regions where CSG activities have been underway during the past decade; therefore, sufficient data probably exists to undertake a study of the subsidence as a result of past CSG activities. One region suitable for such a study is the Camden region (near Campbeltown) SW of Sydney, where several years of images are available from the ERS1, ERS2 and ENVISAT SAR satellite missions. There is also a CORSnet-NSW site located within 3 km of some of the CSG drill sites.

6. Uncertainties, unknowns and research gaps in relation to measuring and monitoring subsidence, especially in relation to CSG activities

There are many case studies that provide clear examples of the types of deformation patterns that have been detected and quantified in relation to subsidence caused by mining and resource extraction activities, but not yet for subsidence related to CSG activities. We did not find any published studies that state that CSG activities do not cause subsidence, so this remains an open question. However, it was not in the brief of this report to discuss whether CSG activities cause subsidence but whether any related subsidence could be detected and, if so, by what means.

There is no doubt that several well-established observation techniques can be used to estimate subsidence. To determine which technique would provide the most cost-effective means of quantifying the deformation, it is necessary to know the spatial extent of the likely deformation field and the expected magnitude of the deformation. Both of these could be predicted in advance of the commencement of mining activity if some of the parameters of the mining activity were known:

1. The magnitude of changes of the gas/water resources;
2. The spatial location – including depth – of the resources;
3. The anticipated time line of the mining activity;
4. The geological structure of the region to be mined.

With such information, it would be possible to generate numerical models to represent the mining activity, from which predictions of likely surface deformation could be made. The predictions could then be used to design an appropriate subsidence-monitoring programme, including baseline measurements. Given that this information was not available during the preparation of this report, no predictions have been made concerning likely subsidence effects.

The process of monitoring deformation using GPS, tiltmeters, LiDAR and InSAR is well understood and there is little risk in using established analysis techniques. A substantial risk exists at present in terms of relying upon space-borne InSAR owing to the current lack of an active C-band or L-band space-borne sensor. This risk would diminish upon successful launch of ALOS-2 and/or Sentinel-1, both scheduled for late 2013. However, the lack of currently active L-band and C-band sensors means that it is unlikely that baseline measurements using InSAR can be made until the proposed missions are launched and active.

7. References

Ackermann, F., (1999) Airborne laser scanning present status and future expectations. ISPRS Journal of Photogrammetry and Remote Sensing 54 (1), 64– 67.

Amelung, F., Galloway D.L., Bell J.W., Zebker H.A., and Laczniak R.J., (1999) Sensing the ups and downs of Las Vegas: InSAR reveals structural control of land subsidence and aquifer-system deformation, *Geology* 27:483–486.

Antonello, G., Casagli, N., Farina, P., Leva, D., Nico, G., Sieber, A.J., Tarchi, D., (2004) Ground-based SAR interferometry for monitoring mass movements, Landslides, 1, 21-28.

Bamler, R., Hartl P., (1998) Synthetic aperture radar interferometry, Inverse Prob 14(4):R1.

Berardino, P., Fornaro G., Lanari R., Sansosti E., (2002) A new algorithm for surface deformation monitoring based on small baseline differential SAR interferograms, IEEE Trans Geosci Remote Sens 40(11):2375–2383. doi:10.1109/tgrs.2002.803792.

Bevis, M., and 21 others, (2005) The B4 Project: Scanning the San Andreas and San Jacinto fault zones: Eos (Transactions, American Geophysical Union), v. 86, fall meeting supplement, abs. H34B–01.

Burgmann, R., Rosen, P.A., Fielding, E.J. (2000) Synthetic aperture radar interferometry to measure Earth's surface topography and its deformation, *Annual Review of Earth and Planetary Sciences* **28**: 169–209, doi:10.1146/annurev.earth.28.1.169

Carter, W.E., Shrestha, R.L., and Slatton, K.C., (2007) Geodetic laser scanning: Physics Today, v. 60, no. 12, p. 41–47, doi:10.1063/1.2825070.

Casagli, N., Luzi G., Fanti R., Gigli G., Leva D., (2013) Integrating radar and laser-based remote sensing techniques for monitoring structural deformation of archaeological monuments Deodato Tapete, Journal of Archaeological Science, 40, p176 -189.

Chapman, B., Hensley S., and Lou Y., (2011) The JPL UAVSAR, *ASF News and Notes*, vol. 7, no. 1.

Cigna, F., Osmano B., Cabral-Cano E., Dixon T.H., Ávila-Olivera J.A., Garduño-Monroy V.H., DeMets C., Wdowinski S., (2012) Monitoring land subsidence and its induced geological hazard with Synthetic Aperture Radar Interferometry: A case study in Morelia, Mexico, Remote Sensing of Environment, 117, p. 146-161.

Davis, E., S. Marsic and W Roadarmel (2008) Deformation monitoring through multi-platform integration, 13th FIG Symposium on Deformation Measurement and Analysis, Lisbon, 12-15 May.

DeLong, S.B., Hilley, G.E., Rymer, M.J., and Prentice, C., (2010) Fault zone structure from topography: Signatures of en echelon fault slip at Mustang Ridge on the San Andreas fault, Monterey County, California: Tectonics, v. 29, doi:10.1029/2010TC002673.

El-Sheimy, N., Valeo, C., and Habib, A., (2005) Digital terrain modeling: Acquisition, manipulation, and applications: Boston, Massachusetts, Artech House, 257 p.

Farr, T.G., et al., (2007) The Shuttle Radar Topography Mission, Rev. Geophys., 45, RG2004, doi:10.1029/2005RG000183.

Featherstone, W.E., M.S. Filmer, N.T. Penna, L.M. Morgan and A. Schenk, Anthropogenic land subsidence in the Perth Basin: challenges for its retrospective geodetic detection, *J .Roy. Soc. West Aus*., 95, 53-62.

Ferretti A, Prati C, Rocca F., (2001) Permanent scatterers in SAR interferometry. IEEE Trans Geosci Remote Sens 39(1):8–20. doi:10.1109/36.89866.

Flood, M. and Gutelius, B., (1997) Commercial implications of Topographic Terrain Mapping Using Scanning Airborne Laser Radar, Photogrammetric Engineering and Remote Sensing 4, p 327-366.

Gruen, A., Akca, D., (2005) Least squares 3D surface and curve matching, ISPRS Journal of Photogrammetry and Remote Sensing, 59, 151-174.

Hanssen, R.F., (2001) Radar Interferometry: Data Interpretation and Error Analysis, Kluwer Academic Publishers.
Harding, D., (2000) Principles of Airborne Laser Altimeter Terrain Mapping, NASA Goddard Space Flight Center.
Hensley, S., Wheeler K., Sadowy G., Miller T., Shaffer S., Muellerschoen R., Jones C., Zebker H., Madsen S., and Rosen P., (2005) Status of a UAVSAR Designed for Repeat Pass Interferometry for Deformation Measurements, Microwave Symposium Digest, 2005 IEEE MTT-S International, vol. 3, pp. 1453-1456.
Hiatt, M.E. (2002). Sensor Integration Aids Mapping at Ground Zero. Photogrammetric Engineering and Remote Sensing, 68, 877-879.
Hilley, G.E., DeLong, S., Prentice, C., Blisniuk, K., and Arrowsmith, J.R., (2010) Morphologic dating of fault scarps using airborne laser swath mapping (ALSM) data: Geophysical Research Letters, v. 37, doi:10.1029/2009GL042044.
Hobbs, P., Humphreys, B., Rees, J., Tragheim, D., Jones, L., Gibson, A., Rowlands, K., Hunter, G. & Airey, R. (2002). Monitoring the role of landslides in 'soft cliff' coastal recession. In: Instability Planning and Management. (Eds, McInnes, R.G. and Jakeways, J.) Thomas Telford, Isle of Wight, 589-600.
Hooper, A, Bekaert D, Spaans K, Arıkan M., (2012) Recent advances in SAR interferometry time series analysis for measuring crustal deformation. Tectonophysics 514–517:1–13. doi:10.1016/j.tecto.2011.10.013
Hudnut, K.W., Borsa, A., Glennie, C., and Minster, J.-B., (2002) High-resolution topography along surface rupture of the 16 October 1999 Hector Mine, California, earthquake (Mw 7.1) from airborne laser swath mapping: Seismological Society of America Bulletin, v. 92, p. 1570–1576, doi:10.1785/0120000934.
Hunter, G., Pinkerton, H., Airey, R. & Calvari, S. (2003). The application of a long-range laser scanner for monitoring volcanic activity on Mount Etna. Journal of Volcanology and Geothermal Research, 123, 203-210.
Jones, L.D. (2006), Monitoring landslides in hazardous terrain using terrestrial LiDAR: an example from Montserrat: Quarterly Journal of Engineering Geology and Hydrogeology, v. 39, 371-373.
Kampes, B.M., (2006) Radar Interferometry. Persistent Scatterer Technique, vol 12. Remote sensing and digital image processing, Springer
Leblanc, M., P. Tregoning, G. Ramillien, S. Tweed, A. Fakes (2009) Basin scale, integrated observations of the early 21st Century multi-year drought in southeast Australia, *Water Resources Res.,* 45, W04408, doi:10.1029/2008WR007333.
Lee, J., B. Strovers, and V. Lin, (2007) C-20A/GIII Precision Autopilot development in support of NASAs UAVSAR program, In Proceeding of the NASA Science Technology Conference 2007, Greenbelt, Maryland, NASA.
Lundgren, P, Usai S, Sansosti E, Lanari R, Tesauro M, Fornaro G, Berardino P., (2001) Modeling surface deformation observed with synthetic aperture radar interferometry at Campi Flegrei caldera. J Geophys Res 106((B9)):19355–19366. doi:10.1029/2001jb000194.
Luzi, G., (2010) Ground based SAR interferometry: a novel tool for geoscience. In: Imperatore, P., Riccio, D. (Eds.), Geoscience and Remote Sensing, New Achievements, Intech, pp. 1-26.
Massonnet, D, Rossi M, Carmona C, Adragna F, Peltzer G, Feigl K, Rabaute T., (1993) The displacement field of the Landers earthquake mapped by radar interferometry. Nature 364(6433):138–142
Massonnet, D., Feigl, K. L., (1998) Radar interferometry and its application to changes in the earth's surface, *Rev. Geophys.* **36** (4): 441–500, doi:10.1029/97RG03139.
McHugh, E.L., Long, D.G., Sabine, C., (2006) Applications of Ground-based Radar to Mine Slope Monitoring, 12 pp. http://www.cdc.gov/niosh/mining/pubs/pdfs/aogbr.pdf.
Monserrat, O., Crosetto, M., (2008) Deformation measurement using terrestrial laser scanning data and least squares 3D surface matching. ISPRS J. Photogramm. Remote Sens. 63, p142-154.

Mora, O, Mallorqui J.J., Broquetas A., (2003) Linear and nonlinear terrain deformation maps from a reduced set of interferometric SAR images. IEEE Trans Geosci Remote Sens 41(10):2243–2253.

Ng, A.H.-M., L. Ge, Y. Yan, X. Li, H.C. Chang, K. Zhang, C. Rizos, (2010) Mapping accumulated mine subsidence using small stack of SAR differential interferograms in the Southern coalfields of New South Wales, Australia, Engineering Geology 115, p1–15.

Olmsted, C., (1993) Alaska SAR Facility Scientific SAR User's Guide (ASF-SD-003), Alaska Synthetic Aperture Radar Facility.

Oskin, M.E., Le, K., and Strane, M.D., (2007) Quantifying fault-zone activity in arid environments with highresolution topography: Geophysical Research Letters, v. 34, doi:10.1029/2007GL031295.

Oskin, M.E., Gold, P.O., Hinojosa, A., Arrowsmith, J.R., Elliott, A.J., Taylor, M.H., Herrs, A.J., Sartori, M., Gonzalez-Garcia, J.J., Gonzalez, A., Kreylos, O., and Cowgill, E., (2010) Airborne and terrestrial LiDAR imaging and analysis of the 4 April 2010 El Mayor–Cucupah earthquake rupture: American Geophysical Union, fall meeting 2010, abs. T35B–2135.

Oskin, M.E., Arrowsmith, J.R., Hinojosa, A.C., Elliott, A.J., Fletcher, J.M., Fielding, E.J., Gold, P.O., Garcia, J.J.G., Hudnut, K.W., Liu-Zheng, J., and Teran, O.J., (2012) Near-field deformation from the El Mayor–Cucupah earthquake revealed by differential LiDAR: Science, v. 335, p. 702–705, doi:10.1126/science.1213778.

Peltzer, G, Rosen P., (1995) Surface Displacement of the 17 May 1993 Eureka Valley, California, Earthquake Observed by SAR Interferometry. Science 268(5215):1333–1336. doi:10.1126/science. 268.5215.1333.

Perissin, D., Prati C.,Rocca F., and Wang T., (2009) PSInSAR analysis over the three gorges dam and urban areas in china. Urban Remote Sensing Event, 2009 Joint, pages 1–5.

Prati C, Ferretti A, Perissin D., (2010) Recent advances on surface ground deformation measurement by means of repeated space-borne SAR observations. J Geodyn 49(3–4):161–170. doi:10.1016/j.jog.2009.10.011.

Prentice, C.S., Crosby, C.J., Whitehill, C.S., Arrowsmith, J.R., Furlong, K.P., and Phillips, D.A., (2009) Illuminating northern California's active faults: Eos (Transactions, American Geophysical Union), v. 90, no. 7, p. 55–56, doi:10.1029/2009EO070002.

Poulton, C.V.L., Lee, J.R., Jones, L.D., Hobbs, P.R.N., and Hall, M. 2006. Preliminary investigation into monitoring coastal erosion using terrestrial laser scanning: case study at Happisburgh, Norfolk, UK: Bulletin of the Geological Society of Norfolk, 56, 45-65. http://nora.nerc.ac.uk/214/

Rodriguez, E., Morris C.S, Belz J.E., Chapin E.C., Martin J.M., Daffer W., Hensley S., (2005) An assessment of the SRTM topographic products, Technical Report JPL D-31639, Jet Propulsion Laboratory, Pasadena, California, 143 pp.

Rosen, P.A, S. Hensley K. Wheeler, G. Sadowy, T. Miller, S. Shaffer, R. Muellerschoen, C. Jones, H. Zebker (2006) UAVSAR : a new NASA airborne SAR system for science and technology, IEEE Radar Conference, Verona, New York, April 24-27, 2006.

Rowlands, K., Jones, L. & Whitworth, M. (2003). Photographic Feature: Landslide Laser scanning: a new look at an old problem. Quarterly Journal of Engineering Geology, 36, 155-158.

Sansosti ,E., Casu F., Manzo M., Lanari R., (2010) Space-borne radar interferometry techniques for the generation of deformation time series: an advanced tool for Earth's surface displacement analysis. Geophys Res Lett 37(20):L20305. doi:10.1029/2010gl044379

Schmidt, D.A, Burgmann R., (2003) Time-dependent land uplift and subsidence in the Santa Clara valley, California, from a large interferometric synthetic aperture radar data set. J Geophys Res 108(B9):2416. doi:10.1029/2002jb002267

Shan, S., Bevis, M., Kendrick, E., Mader, G.L., Raleigh, D., Hudnut, K., Sartori, M., and Phillips, D., (2007) Kinematic GPS solutions for aircraft trajectories: Identifying and minimizing systematic height errors associated with atmospheric propagation delays: Geophysical Research Letters, v. 34, L23S07, doi:10.1029 /2007GL030889.

Simons, M, Rosen P.A., (2007) 3.12 - Interferometric synthetic aperture radar geodesy. In: Gerald S (ed) Treatise on geophys. Elsevier, Amsterdam, pp 391-446

Tarchi, D., H. Rudolf, G. Luzi, L. Chiarantini, P. Coppo, and A.J. Sieber. (1999) Sar interferometry for structural changes detection: a demonstration test on a dam. Geoscience and Remote Sensing Symposium, 1999. IGARSS '99 Proceedings. IEEE 1999 Internationa, 3:1522–152.

Tomas R., Romero R., Mulas J., Marturia J.J., Mallorquı J.J., Lopez-Sanchez J.M., Herrera G., Gutierrez F., Gonzalez P.J., Fernandez J., Duque S., Concha-Dimas A., Cocksley G., Castaneda C., Carrasco D., Blanco P., (2013), Radar interferometry techniques for the study of ground subsidence phenomena: a review of practical issues through cases in Spain, Environ Earth Sci, doi 10.1007/s12665-013-2422-z.

Tregoning, P. and C. Watson (2009) Atmospheric effects and spurious signals in GPS analyses, *J. Geophys. Res.,* 114, B09403, doi:10.1029/2009JB006344

Tregoning, P., C. Watson, G. Ramillien, H. McQueen and J. Zhang (2009) Detecting hydrologic deformation using GRACE and GPS, *Geophys. Res. Lett.* 36, L15401, doi:10.1029/2009GL038718.

Tregoning, P., R. Burgette, S.C. McClusky, S. Lejeune, C.S. Watson and H. McQueen (2013), A decade of horizontal deformation from great earthquakes, *J. Geophys. Res.*, 118, doi:10.1029/jgrb.50154.

Van der Kooij, M. and D. Mayer. (2002) The application of satellite radar interferometry to subsidence monitoring in the belridge and lost hills fields, California. volume 1 of Geoscience and Remote Sensing Symposium, 2002. IGARSS '02. 2002 IEEE International, pages 201– 202.

Wadge, G., Webley, P.W., James, I.N., et al., (2002) Atmospheric models, GPS and InSAR measurements of the tropospheric water vapor field over Mount Etna, Geophysical Research Letters 29 (19), 11/1–11/4.

Watson, C.S., R. Burgette, P. Tregoning, N. White, J. Hunter, R. Coleman, R. Handsworth and H. Brolsma, (2010) Twentieth Century constraints on sea level change and earthquake deformation at Macquarie Island, *Geophys. J. Int.* ,doi:10.1111/j.1365-246X.2010.04640.x

Werner, C., Wegmuller U, Strozzi T, Wiesmann A., (2003) Interferometric point target analysis for deformation mapping. In: Geoscience and remote sensing symposium, IGARSS '03. Proceedings. 2003 IEEE International, 21–25 July 2003 pp 4362–4364 vol.4367. doi:10.1109/igarss.2003.1295516

Wiley, C.A., (1985) Synthetic Aperture Radars: A Paradigm for Technology Evolution, IEEE Transactions on Aerospace and Electronic Systems, v. AES-21, n. 3, pp 440–443.

Williams, S., Bock, Y., Fang, P., (1998) Integrated satellite interferometry: tropospheric noise, GPS estimates and implications for interferometric synthetic aperture radar products, Journal of Geophysical Research 103 (B11), 27,051–27,067.

Xu, C., Wang H., Ge L., Yonezawa C., Cheng P., (2006) InSAR tropospheric delay mitigation by GPS observations: A case study in Tokyo area, Journal of Atmospheric and Solar-Terrestrial Physics 68 (2006) 629–638.